Invited Feature Article

Surface-Bound Soft Matter Gradients

Jan Genzer* and Rajendra R. Bhat†

Department of Chemical & Biomolecular Engineering, North Carolina State University, Raleigh, North Carolina 27695-7905

Received October 24, 2007. In Final Form: December 2, 2007

This feature article describes the progress realized over the past half century in the field of surface-bound gradient structures created on or from soft materials (oligomers and/or polymers), or those enabling the study of the behavior of soft materials. By highlighting our work in the field and accounting for the contribution of other groups, we emphasize the exceptional versatility of gradient assemblies in facilitating fast screening of physicochemical phenomena, acting as "recording media" for monitoring a process, and playing a key role in the design and fabrication of surface-bound molecular and macromolecular motors capable of directing a transport phenomenon.

Introduction

The past few decades witnessed major advances in developing methods for decorating material surfaces with chemical or physical patterns. Various lithographic techniques, including soft lithography[1] and dip-pen lithography,[2] have been invented to impart surfaces with 2D and 3D motifs of nanometer to centimeter dimensions. Although useful for endowing the substrates with well-defined chemical and/or physical "blueprints" of diverse shapes and dimensions, these techniques typically produce sharp boundaries between the distinct chemical or physical regions on the substrate. Yet, for some applications it is desirable that the physicochemical nature of those patterns possesses spatiotemporal character (i.e., one that changes gradually over a certain length in space and may even evolve in time). This can be accomplished by using material gradients—structures, defined broadly as molecular or macromolecular patterns with a spatiotemporal change of at least one of their physicochemical characteristic. Over the past half century, gradient surfaces have played a pivotal role in numerous aspects of materials research. Being a subset of the high-throughput screening methodologies, gradient assemblies have facilitated the fast screening of physicochemical phenomena, enabled the fabrication of material structures that would have been difficult to manufacture otherwise, acted as recording media for monitoring a given process, and played a key role in designing and fabricating surface-bound "engines" capable of acting as molecular and macromolecular motors and thus drove and/or directed a given transport phenomenon.

On the basis of their preparation method, approaches to create a substrate-bound gradient can be broadly classified into two major categories: (1) bottom up and (2) top down. In the bottom-up techniques, gradients are designed and built on a parent substrate by gradually depositing the gradient building blocks (monomers, oligomers, polymers, etc.) via either naturally occurring (diffusion, propagating front, etc.) or man-made (i.e., controlled sample dipping into a solution, deposition-dependent evaporation, or external field-assisted) deposition methods. In the top-down methodologies, a parent material, typically a flat substrate, is progressively modified chemically or physically. Different techniques can be combined in sequential steps, thereby fabricating complex gradient geometries exhibiting a gradual variation of two (or more) properties of the newly generated surface in two (or more) independent directions. In addition to the substrate-bound gradients, methods have been developed that enable the formation of substrate-free gradient structures that eventually get imprinted onto a support. An example of such a configuration involves a chemical gradient formed inside a microfluidic chip (discussed in detail below), where the chemistry variation occurs across the flow direction of a fluid.

Most gradients fabricated today possess static character. That is, the variation of a given physicochemical property on the substrate has been defined during the time of the gradient creation and is fixed. As will be discussed in detail later, such substrates are suited for screening material properties (i.e., adsorption of nanoparticles or proteins) or even driving a certain dynamical phenomenon (i.e., moving liquids across surfaces). In some applications, however, it is convenient to decorate surfaces with gradients whose properties change with time as a result of a response to the variation of some external stimulus (temperature, pH, external electrical field, flow, etc.). Spatiotemporal variation of this external field on the substrate leads to a gradient in the substrate physicochemical property, typically a gradient in surface energy, and can thus be used to drive a given phenomenon. Such responsive "dynamical gradients" offer exciting new opportunities for generating "smart materials" and "surface-bound engines" capable of directing a given phenomenon (i.e., motion of liquids, gels, particles, living cells on the substrate, mixing liquids, causing temporal variation in the substrate roughness for optical or transport purposes, and many others). We discuss some examples of this type of gradient later in the text.

We offer gradient structure classification based on a few key attributes. Those are depicted pictorially in Figure 1. It has to be stressed that such a division, while perhaps illustrative, may be a bit simplistic. Toward this end, just about any material

* Corresponding author. E-mail: jan_genzer@ncsu.edu. Phone: +1-919-515-2069.

† Current address: Becton Dickinson (BD) Technologies, Research Triangle Park, North Carolina 27709.

(1) Whitesides, G. M.; Xia, Y. *Annu. Rev. Mater. Sci.* **1998**, *28*, 153−184.

(2) Piner, R. D.; Zhu, J.; Xu, F.; Hong, S.; Mirkin, C. A. *Science* **1999**, *283*, 661−663.

10.1021/la7033164 CCC: $40.75 © 2008 American Chemical Society
Published on Web 01/26/2008

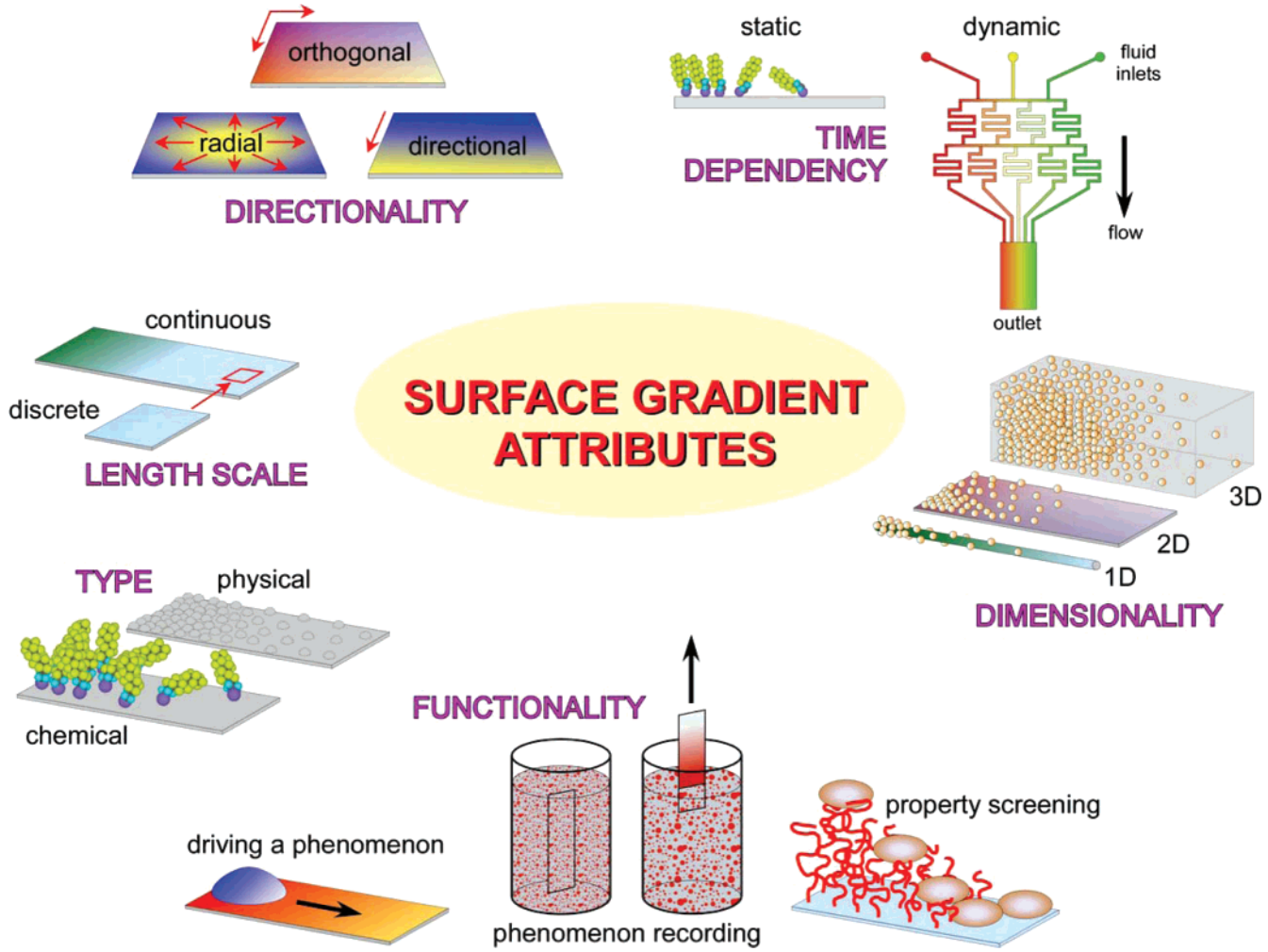

Figure 1. Schematic of the various attributes of surface-bound gradients.

gradient can belong to more than just one category. For instance, let us consider a case of a gradient comprising assemblies of nanoparticles distributed in a gradual fashion on a flat substrate (2D dimensionality category in Figure 1). From the point of view of the nanoparticles, such a structure consists of position-dependent arrangement of nanoparticles on surfaces. Such a particle array can be realized by generating a chemical gradient of some adhesion precursors on surfaces (chemical type category in Figure 1), which can possess various directionalities (directionality category in Figure 1). Depending on the length scale of interest, these gradients can be continuous or discontinuous (length scale category in Figure 1). Finally, the distribution of nanoparticles in a gradual fashion across surfaces causes variation in some physicochemical property, say, light absorption, scattering, and so forth. As such, these gradient composites are expected to possess position-dependent functionality.

Continuous or discrete molecular gradients have witnessed major developments in combinatorial chemistry and materials science, including the design and discovery of catalysts and drugs, thus leading to rapid technological developments with improved efficiency and lower research and production cost.[3,4] They also facilitated the development of new analytical approaches and measurement tools.[5−9] The progress in generating and utilizing material gradient surfaces has been summarized in several review articles.[10−20] Because of the rapid development of new gradient methodologies conceived and put into practice over the past few years, the time is right to update the reader on the latest developments in the field of soft material gradients.

(3) van Dover, R. B.; Scheemeyer, L. F.; Fleming, R. M. *Nature* **1998**, *392*, 162−164.
(4) Jandeleit, B.; Schaefer, D. J.; Powers, T. S.; Turner, H. W.; Weinberg, W. H. *Angew. Chem., Int. Ed.* **1999**, *38*, 2494−2532.
(5) Genzer, J.; Fischer, D. A.; Efimenko, K. *Appl. Phys. Lett.* **2003**, *82*, 266−268
(6) Fischer, D. A.; Efimenko, K.; Bhat, R. R.; Sambasivan, S.; Genzer, J. *Macromol. Rapid Commun.* **2004**, 25, 141−149
(7) Stafford, C. M.; Harrison, C.; Beers, K. L.; Karim, A.; Amis, E. J.; Vanlandingham, M. R.; Kim, H.-C.; Volksen, W.; Miller, R. D.; Simonyi, E. E. *Nat. Mater.* **2004**, *3*, 545−550
(8) Julthongpiput, D.; Fasolka, M. J.; Zhang, W.; Nguyen, T.; Amis, E. J. *Nano Lett.* **2005**, *5*, 1535−1540.
(9) Potyrailo, R.; Hassib, L. *Rev. Sci. Instrum.* **2005**, *76*, 062225-1−062225-9.
(10) Elwing, H.; Gölander, C.-G. *Adv. Colloid Interface Sci.* **1990**, *32*, 317−339.
(11) Ruardy, T. G.; Schakenraad, J. M.; van der Mei, H. C.; Busscher, H. J. *Surf. Sci. Rep.* **1997**, *29*, 1−30.
(12) Genzer, J. Molecular Gradients: Formation and Applications in Soft Condensed Matter Science. In *Encyclopedia of Materials: Science and Technology*; Buschow, K. H. J., Cahn, R. W., Flemings, M. C., Ilschner, B., Kramer, E. J., Mahajan, S., Eds.; Elsevier: Amsteradm, 2002; pp 1−8.
(13) Amis, E. J.: Xiang, X.-D.; Zhao, J.-C. *MRS Bull.* **2002**, *27*, 295−300 and accompanying articles in the same issue.
(14) Genzer, J.; Bhat, R.; Wu, T.; Efimenko, K. Molecular Gradient Nanoassemblies. In *Encyclopedia of Nanoscience and Nanotechnology*; Nalwa, H. S., Ed.; American Scientific Publishers: Stevenson Ranch, CA, 2003; Vol. 5, pp 663−676.
(15) Genzer, J. *J. Adhes.* **2005**, *81*, 417−435.
(16) Wu, T.; Tomlinson, M.; Efimenko, K.; Genzer, J. *J. Mater. Sci.* **2003**, *38*, 4471−4477.
(17) Bhat, R. R.; Tomlinson, M. R.; Genzer, J. *J. Polym. Sci., Polym. Phys. Ed.* **2005**, *43*, 3384−3394.
(18) Bhat, R. R.; Tomlinson, M. R.; Wu, T.; Genzer, J. *Adv. Polym. Sci.* **2006**, *198*, 51−124.
(19) Lee, H. B.; Kim, M. S.; Chi, Y. H.; Khang, G.; Lee, J. H. *Polym. Korea* **2005**, *29*, 423−432.

For the past few years, our research group has had an interest in generating, investigating, and utilizing gradient-based surfaces. To this end, we have developed novel methods leading to the formation of substrate-bound oligomer and polymer gradients on substrates. Subsequently, these gradient patterns were employed to studying several phenomena, including the formation of self-assembled monolayers, the kinetics of polymerization from substrates, the formation of nanoparticle−polymer (or oligomer) composites, and monitoring the adsorption of proteins and cells on polymer brushes just to name a few. Rather than separately describing the individual efforts that we have made to the field of gradient surfaces, we have opted to interject them in the context of the overall progress being accomplished in the field. The narrative that follows is structured such that we discuss our work and that of others in terms of chief attributes of gradient surfaces. We discuss a few selected technologies leading to the formation of such gradient surfaces and illustrate the applications of gradient-based surfaces. We restrict ourselves to the discussion of material gradients formed from or onto soft (i.e., polymeric or oligomeric) materials and those that have been utilized to investigate the behavior of various soft materials. Readers interested in a broader aspect of combinatorial/high-throughput materials science are directed to the plethora of monographs available on this subject.

1. Gradient Type

Gradients can be classified into many categories depending on their physicochemical nature. For this discussion, gradients will be described in terms of either their chemical composition (chemical gradients) or their resultant physical properties (physical gradients), though these imposed classes are not mutually exclusive in a single material. What follows is a discussion of the top-down and bottom-up approaches to create both classes of gradients.

1.1. Chemical Gradients. Conventional (chemical) gradients involve the gradual variation of one or more chemistries on a substrate. A variation in the density and/or the chemical nature of the surface-anchored species leads to a position-dependent variation in the wettability of the surface (Figure 2). For example, two chemically distinct macromolecular brushes may be grafted to a substrate so that the grafting densities of each vary in directions that are either opposite or orthogonal to each other, as will be discussed later. Clearly, having a chemical gradient present on a surface may alter many properties of the final material (i.e., in addition to the wettability of a surface, optical, electrical, and other characteristics can vary as a function of the position on the substrate (and maybe time)). These resulting variations in physical properties, however, will be discussed in section 1.2 on physical gradients. Also important to the discussion of chemical gradients is the dimensionality of the gradient. Hence, this section is organized by the dimensionality of the gradient-forming technique (2D, 3D) whereas a more thorough discussion on the topic of dimensionality will be postponed until section 2. The generation of chemical or physical gradients involves invoking one or more of the many existing bottom-up or top-down approaches. Figure 2 pictorially depicts a few selected examples. The gradient is typically formed by either (1) time-dependent exposure of the substrate to some modifying source or (2) scanning the modifying source across the substrate.

Several top-down methods have been developed that modify the surface of a matrix material (typically polymeric) to prepare a 2D chemical gradient. These include but are not limited to (1) chemical treatment of a polymer matrix coupled with gradual immersion of the sample in the modifying liquid (e.g., hydrolysis of poly(vinylene carbonate) to produce poly(hydroxyl methylene) in an alkaline solution),[21] (2) hyperthermal polyatomic ion deposition with position-dependent fluence (e.g., modification of poly(methyl methacrylate) (PMMA) via $C_3F_5^+$ ions),[22] (3) exposure of a polymer surface to a radio-frequency plasma discharge while simultaneously moving a shutter over the polymer surface,[23,24] and (4) corona discharge on a polymer surface (i.e., treating low-density polyethylene sheets in air with the corona from a knife-type electrode where power to the electrode is increased gradually as the electrode is passed along the surface).[25−28] The latter method has also been used to produce gradients in polymer grafts for poly(acrylic acid)[29] and poly(ethylene glycol) (PEG).[30]

To date, however, most 2D chemical gradients have been formed by bottom-up approaches. Examples include (1) directed deposition of metals (e.g., palladium on cellulose acetate-covered glass using a "shadowing method"),[31] (2) variants of the deposition of organosilanes from liquids,[32,33] (3) vapor deposition of organosilanes,[34,35] (4) interdiffusion of alkanethiols in a polysaccharide matrix,[36−38] (5) electrochemical desorption/adsorption of alkanethiols[39−43] and peptides,[44] (6) self-assembled monolayer (SAM) deposition with selective and position-dependent removal of adsorbed alkanethiols and replacement with others (so-called replacement lithography),[45] (7) gradual immersion of a vertically positioned gold-coated substrate into a solution of one thiol (with, say, a hydrophilic end-group) followed by subsequent immersion into a solution of another thiol (with, say, a hydrophobic end-group),[46] (8) application of the Langmuir−Blodgett rotating-

(20) Morgenthaler, S.; Zink, C.; Spencer, N. D. *Soft Matter*, submitted for publication, 2007.

(21) Ueda-Yukoshi T.; Matsuda, T. *Langmuir* **1995**, *11*, 4135−4140.
(22) Wijesundara, M. B.; Fuoco, E.; Hanley, L. *Langmuir* **2001**, *17*, 5721−5726.
(23) Pitt, W. G. *J. Colloid Interface Sci.* **1989**, *133*, 223−227.
(24) Spijker, H. T.; Bos, R.; van Oeveren, W.; de Vries, J.; Busscher, H. J. *Colloids Surf., B* **1999**, *15*, 89−97.
(25) Lee, J. H; Kim, H. G.; Khang, G. S.; Lee, H. B.; Jhon, M. S. *J. Colloid Interface Sci.* **1992**, *151*, 563−570.
(26) Lee, J. H.; Kim, H. W.; Pak, P. K.; Lee, H. B. *J. Polym. Sci.: Polym. Chem. A* **1994**, *32*, 1569−1579.
(27) Kim, M. S.; Cho, Y. H.; Lee, S. Y.; Khang, G.; Lee, T. G.; Moon, D. W.; Lee, H. B. *Chem. Lett.* **2006**, *35*, 728−729.
(28) Lee, T. G.; Shon, H. K.; Kim, M. S.; Lee, H. B.; Moon, D. W. *Appl. Surf. Sci.* **2006**, *252*, 6754−6756.
(29) Kim, H. G.; Lee, J. H.; Lee, H. B.; Jhon, M. S. *J. Colloid Interface Sci.* **1993**, *157*, 82−87.
(30) Jeong, B. J.; Lee, J. H.; Lee, H. B. *J. Colloid Interface Sci.* **1996**, *178*, 757−763.
(31) Carter, S. B. *Nature* **1965**, *208*, 1183−1187.
(32) Elwing, H.; Welin, S.; Askendal, A.; Nilsson, U.; Lundström, I. *J. Colloid Interface Sci.*, **1987**, *119*, 203−210.
(33) Gölander, C. G.; Caldwell; K.; Lin, Y.-S. *Colloids Surf.* **1989**, *42*, 165−172.
(34) Chaudhury, M. K.; Whitesides, G. M. *Science* **1992**, *256*, 1539−1541.
(35) Genzer, J.; Efimenko, E.; Fischer, D. A. *Langmuir* **2006**, *22*, 8532−8541.
(36) Liedberg, B.; Tengvall, P. *Langmuir* **1995**, *11*, 3921−3827.
(37) Liedberg, B.; Wirde, M.; Tao, Y.-T.; Tengvall, P.; Gelius, U. *Langmuir* **1997**, *13*, 5329−5334.
(38) Lestelius, M.; Enquist, I.; Tengvall, P.; Chaudhury, M. K.; Liedberg, B. *Colloids Surf., B* **1999**, *15*, 57−70.
(39) Terrill, R. H.; Balss, K. M.; Zhang, Y.; Bohn, P. W. *J. Am. Chem. Soc.* **2000**, *122*, 988−989.
(40) Balss, K. M.; Coleman, B. D.; Lansford, C. H.; Haasch, R. T.; Bohn, P. W. *J. Phys. Chem. B* **2001**, *105*, 8970−8978.
(41) Plummer, S. T.; Bohn, P. W. *Langmuir* **2002**, *18*, 4142−4149.
(42) Balss, K. M.; Fried, G. A.; Bohn, P. W. *J. Electrochem. Soc.* **2002**, *149*, C450−C455.
(43) Balss, K. M.; Cuo, T. C.; Bohn, P. W. *J. Phys. Chem. B* **2003**, *107*, 994−1000.
(44) Plummer, S. T.; Wang, Q.; Bohn, P. W.; Stockton, R.; Schwartz, M. A. *Langmuir* **2003**, *19*, 7528−7536.
(45) Fuierer, R. R.; Carroll, L.; Feldheim, D. L.; Gorman, C. B. *Adv. Mater.* **2002**, *14*, 154−157.
(46) Morganthaler, S.; Lee, S.; Zürcher, S.; Spencer, N. D. *Langmuir* **2003**, *19*, 10459−10462.

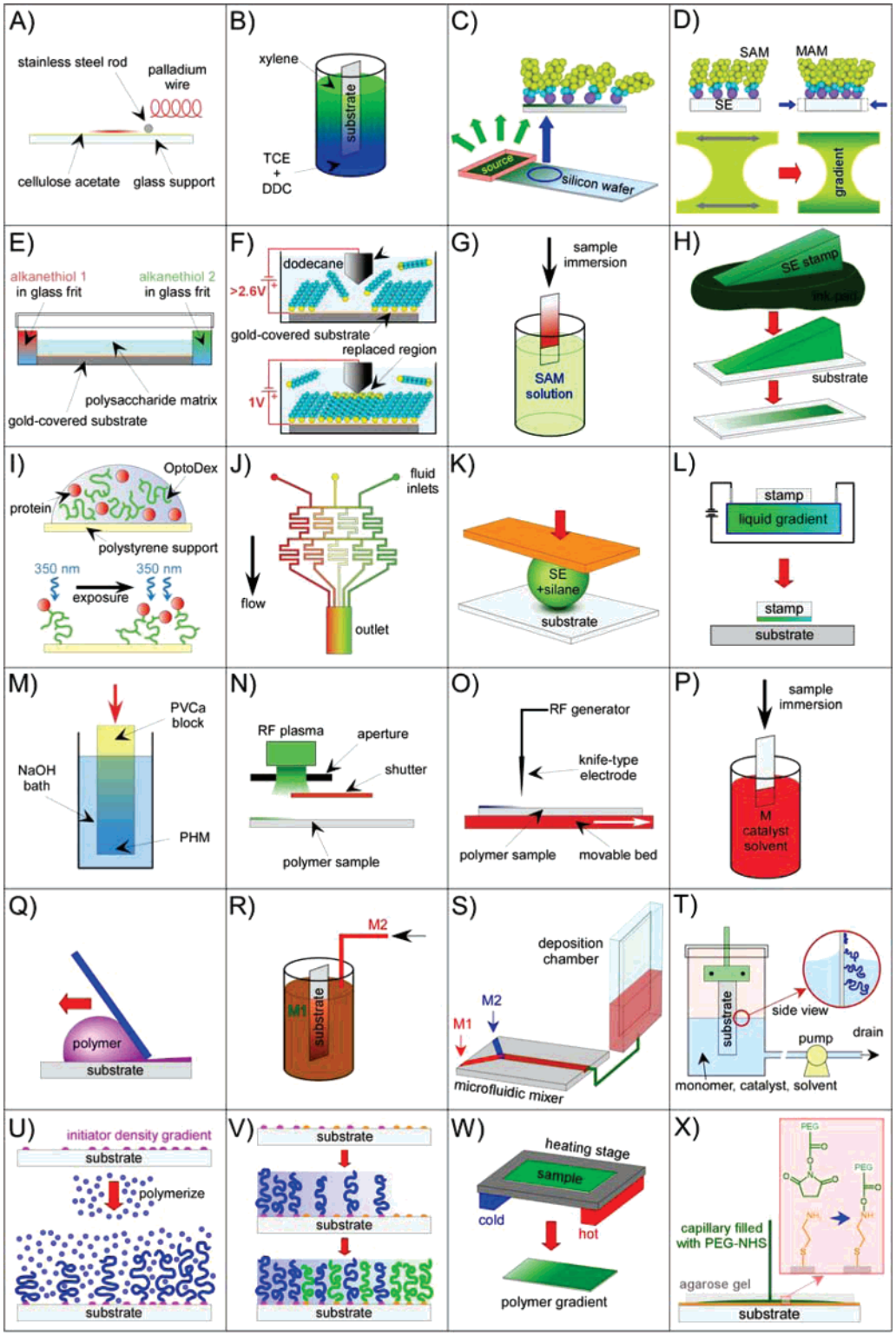

Figure 2. Various methods of creating molecular and macromolecular gradients: (A) deposition of palladium;[31] (B) liquid diffusion of organosilanes;[32] (C) vapor diffusion of organosilanes;[34] (D) depositing self-assembled monolayer on top of a mechanically predeformed substrate;[75] (E) diffusion of alkanethiols in a polysaccharide matrix;[36] (F) replacement lithography of alkanetiols;[45] (G) immersion technique applied to self-assembled monolayers;[46] (H) printing alkanethiols from stamps of variable thickness;[49] (I) gradients of proteins by means of heterobifunctional photolinkers;[60] (J) solution and surface gradient using microfluidics;[78] (K) deposition of organosilanes by means of silicone elastomer stamps with different curvatures;[48] (L) forming a concentration gradient of two charged molecules in a solution and imprinting them onto a stamp, which could then transfer the gradient pattern onto a substrate;[66] (M) hydrolysis of poly(vinylene carbonate);[21] (N) radio frequency plasma discharge;[23] (O) corona discharge;[25] (P) immersion of substrates into polymerization media;[96] (Q) knife-edge coating technology;[85,88] (R) preparing random copolymer brushes by steadily adding a new monomer (M2) to the polymerization mixture containing another monomer (M1);[92] (S) preparing statistical copolymers by the microfluidic mixing of two monomers followed by chamber filling method;[93] (T) solution draining method for preparing polymer brushes;[130] (U) forming a molecular gradient of an initiator on a substrate followed by grafting-from polymerization;[126,127] (V) opposite grafting density counter gradients of two polymers formed by sequential grafting from two different set of initiators;[131] (W) grafting-onto method in conjunction with temperature gradient heating of the substrate;[120] and (X) immobilization of PEG by diffusion and grafting.[124]

transfer method,[47] (9) deposition of organosilanes by means of silicone elastomer (SE) stamps with different curvatures,[48] (10) soaking of thiol precursors into SE stamps with gradients in thickness, causing a gradient uptake of the thiols at different positions along the stamp, and subsequent printing of thiols onto a flat substrate,[49] (11) chemical conversion of SAM molecules with ultraviolet radiation,[50,51] (12) application of soft X-rays,[52,53] (13) deposition of alkanethiol-based molecules across assembled arrays of silica particles (edge-spreading lithography),[54] (14) selective degradation of existing alkanethiol SAMs via photocatalytic lithography and filling of the empty sites on the surface with another thiol molecule,[55] (15) gradually depositing alkanethiols onto rough gold substrates,[56] and (16) layer-by-layer sequential deposition of negatively charged silica nanoparticles and positively charged poly(allylamine hydrochloride) onto flat silica substrates followed by position-dependent UV treatment.[57] In addition to depositing metals or small organic precursors,[58,59] techniques have been developed that enable the deposition of larger organic clusters (i.e., proteins) or nanoparticles (i.e., metals). These involve gradients prepared by (17) using heterobifunctional photolinkers,[60−62] (18) gradually immersing a glass slide modified with poly-L-lysine into a solution of gold particles covered with a protein (e.g., bovine serum albumin, ephrin-A5, or ephrin-B1),[63] (19) mixing solutions of acrylic acid and (Arg-Gly-Asp) (RGD)-modified acrylic acid, depositing them onto substrates treated previously with 3-acryloxypropyl trichlorosilane, and immobilizing with photopolymerization,[64] (20) immobilizing ligands to quinine-terminated alkanethiols (via Diels−Alder reaction) formed by patterning hydroquinone-terminated SAM precursors via UV light across a mask,[65] (21) forming a concentration gradient of two charged molecules in a solution and imprinting them onto a stamp that can transfer the gradient pattern onto a substrate,[66] (22) combining metal transfer onto a polymer substrate with subsequent chemical functionalization of the nonmetalized surface regions,[67] (23) heating of poly(methyl silsesquioxane) films, which leads to the formation of a position-dependent organic/inorganic wettability gradient,[68] (24) immobilization of oligonucleotides on indium tin oxide (ITO) substrates in a microfluidic channel,[69] (25) electrochemical desorption/adsorption of signaling molecules (i.e., epidermal growth factor, EGF),[70] (26) chemical grafting of peptide (i.e., Gly-Arg-Gly-Asp-Ser, GRGDS) onto UVO-modified alkanethiol SAM surfaces,[71] and (27) poly(acryl amide gels) with a gradient of ester groups prepared by interdiffusion and cross-linking[72] membrane material on top of a capillary pore filter by moving a cover slip.[73,74] In addition, a library of other methods has been developed that permit the fabrication of gradient structures involving substrate-grafted polymer assemblies; these are discussed in detail in the forthcoming sections.

Several specialized types of chemical gradients have also been reported. These include functional coatings fabricated on flexible supports, such as SEs made of poly(dimethylsiloxane) networks. The gradient nature is achieved by depositing SAMs on top of a mechanically predeformed substrate[75] or by combination of the vapor deposition methods with substrate deformation.[76,77] Other special cases of 2D chemical gradients are those prepared by the means of liquid mixing in microfluidic channels.[78−84] What distinguishes the latter class of structures from other more conventional gradients is the fact that they are created inside a channel of a microfluidic device rather than by grafting on top of a solid substrate. The formation and characteristics of microfluidic gradients are discussed in section 5 on temporal gradients.

Although some of the work involving the formation of gradients made of peptides, proteins, or other larger molecular clusters may also be considered to be examples of 3D chemical gradients, true 3D chemical gradients are almost exclusively formed by either depositing polymer films onto substrates by (1) "knife-edge coating" technology,[85−88] (2) grafting substrates with macromolecules and controlling the chain grafting density, length, and composition of such surface-tethered modifiers as a function of the position on the substrate,[16−18] or (3) by controlling the

(47) Chen, X.; Hirtz, M.; Fuchs, H.; Chi, L. *Langmuir* **2007**, *23*, 2280−2283.
(48) Choi, S.-H.; Zhang Newby, B.-m. *Langmuir* **2003**, *19*, 7427−7435.
(49) Kraus, T.; Stutz, R.; Balmer, T. E.; Schmid, H.; Malaquin, L.; Spencer, N. D.; Wolf, H. *Langmuir* **2005**, *21*, 7796−7804.
(50) Roberson, S.; Sehgal, A.; Fahley, A.; Karim, A. *Appl. Surf. Sci.* **2003**, *203−204*, 855−858.
(51) Ito, Y.; Heydari, M.; Hashimoto, A.; Cono, T.; Hirasawa, A.; Hori, S.; Kurita, K.; Nakajima, A. *Langmuir* **2007**, *23*, 1845−1850.
(52) Klauser, R.; Chen, C.-H.; Huang, M.-L.; Wang, S.-C.; Chuang, T. J.; Zharnikov, M. *J. Electron Spectrosc. Relat. Phenom.* **2005**, *144−147*, 393−396.
(53) Ballav, N.; Shaporenko, A.; Terfort, A.; Zharnikov, M. *Adv. Mater.* **2007**, *19*, 998−1000.
(54) Geissler, M.; Chalsani, P.; Cameron, N. S.; Veres, T. *Small* **2006**, *2*, 760−765.
(55) Blondiaux, N.; Zürcher, S.; Liley, M.; Spencer, N. D. *Langmuir* **2007**, *23*, 3489−3494.
(56) Yu, X.; Wang, Z.; Kiang, Y.; Zhang, X. *Langmuir* **2006**, *22*, 4483−4486.
(57) Han, J. T.; Kim, S.; Karim, A. *Langmuir* **2007**, *23*, 2608−2614.
(58) Schmitz, C.; Thelakkat, M.; Schmidt, H. W. *Adv. Mater.* **1999**, *11*, 821−826.
(59) Schmitz, C.; Pösch, P.; Thelakkat, M.; Schmidt, H. W. *Phys. Chem. Chem. Phys.* **1999**, *1*, 1777−1781.
(60) Hypolite, C. L.; McLernon, T. L.; Adams, D. N.; Chapman, K. E.; Herbert, C. B.; Hunag, C. C.; Distefano, M. D.; Hu, W.-S. *Bioconjugate Chem.* **1997**, *8*, 658−663.
(61) Caelen, I.; Gao, H.; Sigrist, H. *Langmuir* **2002**, *18*, 2463−2467.
(62) Kipper, M. J.; Kleinma, H. K.; Wang, F. W. *Anal. Biochem.* **2007**, *363*, 175−184.
(63) Krämer, S.; Xie, H.; Gaff, J.; Williamson, J. R.; Tkachenko, A. G.; Nouri, N.; Feldheim, D. A.; Feldheim, D. L. *J. Am. Chem. Soc.* **2004**, *126*, 5388−5395.
(64) Kang, C. E.; Gemeinhart, E. J.; Gemeinhart, R. A. *J. Biomed. Mater. Res. A* **2004**, *71A*, 403−411.
(65) Dillmore, W. S.; Yousaf, M. N.; Mrksich, M. *Langmuir* **2004**, *20*, 7223−7231.
(66) Venkateswar, R. A.; Branch, D. W.; Wheeler, B. C. *Biomed. Microdev.* **2000**, **2**, 255−264.
(67) Bhangale, S. M.; Tjong, V.; Wu, L.; Yakovlev, N.; Moran, P. M. *Adv. Mater.* **2005**, *17*, 809−813.
(68) Liu, H.; Xu, J.; Li, Y.; Li, B.; Ma, J.; Zhang, X. *Macromol. Rapid Commun.* **2006**, *27*, 1603−1607.
(69) Park, S. H.; Krull, U. *Anal. Chim. Acta* **2006**, *564*, 133−140.
(70) Wang, Q.; Bohn, P. W. *Thin Solid Films* **2006**, *513*, 338−346.
(71) Gallant, N. D.; Lavery, C. A.; Amis, E. J.; Becker, M. L. *Adv. Mater.* **2007**, *19*, 965−969.
(72) Brandley, B. L.; Weisz, O. A.; Schnaar, R. L. *J. Biol. Chem.* **1987**, *262*, 6431−6437.
(73) Baier, H.; Bohnoeffer, F. *Science* **1992**, *255*, 472−475.
(74) Rosentreter, S.; Davenport, R. W.; Löschinger, J.; Huf, J.; Jung, J.; Bohnoeffer, F. *J. Neurobiol.* **1998**, *37*, 541−562.
(75) Genzer, J.; Efimenko, K.; Fischer, D. A. *Adv. Mater.* **2003**, *15*, 1545−1547.
(76) Efimenko, K. Genzer, J. *Adv. Mater.* **2001**, *13*, 1560−1563.
(77) Efimenko, K. Genzer, J. *Mater. Res. Soc. Symp. Proc.* **2002**, *710*, DD10.3.1−DD10.3.6.
(78) Jeon, N. L.; Dertinger, S. K. W.; Chiu, D. T.; Choi, I. S.; Stroock, A.; Whitesides, G. M. *Langmuir* **2000**, *16*, 8311−8316.
(79) Caelen, I.; Bernard, A.; Juncker, D.; Michel, B.; Heinzelmann, H.; Delamarche, E. *Langmuir* **2000**, *16*, 9125−9130.
(80) Dertinger, S. K. W.; Chiu, D. T.; Jeon, N. L.; Whitesides, G. M. *Anal. Chem.* **2001**, *73*, 1240−1246.
(81) Dertinger, S. K. W.; Jiang, X. Y.; Li, Z. Y., Murthy, V. N.; Whitesides, G. M. *Proc. Natl. Acad. Sci. U.S.A.* **2002**, *99*, 12542−12547.
(82) Fosser, K. A.; Nuzzo, R. G. *Anal. Chem.* **2003**, *75*, 5775−5782.
(83) Rhoads, D. S.; Nadkarni, S. M.; Song, L.; Voeltz, C.; Bodenschatz, E.; Guan, J.-L. Using Microfluidic Channel Networks to Generate Gradients for Studying Cell Migration. In *Cell Migration: Developmental Methods and Protocols*; Methods in Molecular Biology; Guan, J.-L., Ed.; Humana Press, Inc.: Totowa, NJ, 2004; Vol. 294.
(84) Jiang, X.; Xu, Q.; Dertinger, S. K. W.; Stroock, A. D.; Fu, T.-m.; Whitesides, G. M. *Anal. Chem.* **2005**, *77*, 2338−2347.
(85) Meredith, J. C.; Karim, A.; Amis, E. J. *Macromolecules* **2000**, *33*, 5760−5762.
(86) Meredith, J. C.; Smith, A. P.; Karim, A.; Amis, E. J. *Macromolecules* **2000**, *33*, 9747−9756.
(87) Smith, A. P.; Douglas, J.; Meredith, J. C.; Karim, A.; Amis, E. J. *Phys. Rev. Lett.* **2001**, *87*, 15503-1−15503-4.
(88) Meredith, J. C.; Karim, A.; Amis, E. J. *MRS Bull.* **2002**, *27*, 330−335.

spatial distribution of polymer during adsorption using the so-called "grafting-onto" approach. We will discuss the effects of molecular weight, grafting density of surface-anchored polymers, and adsorbed amount of grafted-onto polymers in the following section pertaining to the gradient dimensionality of the substrate. Here we only briefly mention methods involving chemical composition variation in three dimensions.

Whittle, Alexander, and co-workers reported on the formation of 3D chemical gradients via plasma polymerization. During polymerization, the composition of the plasma feed was changed; concurrently, the deposits were shielded across the substrate.[89−91] Such gradients were subsequently utilized in studying the adsorption of small organic molecules.[90] A large body of work exists on preparing surface-anchored polymers involving so-called "grafting from" polymerization. In this process, the substrate is typically covered by polymerization initiators from which the polymer grows upon immersing such a substrate into the monomer solution (plus some catalyst, depending on the polymerization method used). Xu et al. reported on the formation of surface-anchored statistical copolymers on flat substrates with composition gradients.[92,93] Block copolymer gradients with gradual variation of both block length and the overall polymer molecular weight were also prepared by sequential polymerization of two or three monomers combined with the methods of producing the molecular weight gradient of surface-anchored macromolecules based on either draining a polymerization mixture from the reaction vessel or by gradually dipping the samples into the polymerization media.[94−96]

In addition to the classical wettability gradients, methods have been developed that facilitate the generation of other gradients in liquids that can be deposited onto substrates[97,98] and gradients of selected physicochemical properties, such as those in pH[99−101] and refractive index.[102]

1.2. Physical Gradients. We define physical gradients as structures that possess a gradual variation of some physical property other than wettability. One such property, the substrate modulus (i.e., rigidity of the substrate), has in the past been shown to impact cell motility (so-called durotaxis).[103] Wang and co-workers were among the first groups to create such substrates by interdiffusing mixtures of acrylamide and bis-acrylamide of different compositions.[104] Wong and co-workers later extended the method by creating rigidity gradients by exposing acrylamide and bis-acrylamide solutions (containing a small amount of photoinitiator) to UV light across masks having position-dependent shading.[105] The modulus variation across the samples was assessed by indentation measurement using atomic force microscopy (AFM) and by monitoring the motion of fluorescent beads embedded in the sample. Capitalizing on earlier work by Domingo,[97] Zaari and co-workers achieved microscale control over substrate compliance inside microfluidic channels by mixing two solutions of acrylamide and bis-acrylamide having different compositions and then exposing the mixed fluid to UV light, which cross-linked the liquid precursors into a network.[106]

Another physical property of interest is surface topography/roughness. One of the first attempts to create substrates with a gradual variation of surface roughness was reported by Einaga and co-workers,[107] who fabricated graded-morphology diamond thin films using a simple technique involving chemical vapor deposition (CVD). During the process, the temperature of the substrate was gradually changed by heating one end of the substrate while cooling the other. This setup thus facilitated control of the size of the grains in the film from submicrometer (lower temperature) to ∼10 μm (higher temperature). Tsai and co-workers[108] reported on preparing polymer surfaces with a gradual variation of topography by interdiffusion solutions comprising a mixture of polystyrene (PS), poly(methyl methacrylate) (PMMA), and a diblock copolymer of PS-*b*-PMMA on a substrate. The substrate was chemically grafted with a PS-*r*-PMMA random copolymer whose composition was chosen such that the surface appeared "neutral" to both PS and PMMA.[109] The deposited polymer mixture was swept with a razor blade, thus creating a thickness gradient. Subsequent annealing of the film, sputtering the topmost layer of the film by reactive ion etching, and exposing to UV radiation resulted in cross linking of the PS domains and selective degradation of the PMMA domains. The resulting morphology comprising interdispersed islands with roughness ranging from nanoscopic to microscopic dimensions was used to study the adhesion of fibroblast cells. Lu and co-workers reported on fabricating substrates with gradual roughness variation by first creating a porous polyethylene (PE) sheet using the method described by Erbil and co-workers,[110] followed by placing the substrate onto a heating stage with a temperature gradient ranging from 0 °C to temperatures above the melting point of PE. The morphology changed gradually from porous (close to the cooled end) to smooth (close to the heated end) across the substrate.[111] By analogy to the previous method, Zhang and co-workers reported on fabricating gradient topographical substrates[112] by first assembling PS microspheres onto a flat silicon wafer and placing the substrate onto a heating stage whose temperature ranged from room temperature to 130 °C, well above the glass-transition temperature of PS. After heat treatment, the surface topography evolved from flat (high temperature, at which the spheres melted and formed a continuous layer) to rough (low temperature, where the spheres remained intact) (Figure 3A). Han and co-workers demonstrated the possibility of fabricating surfaces with gradients in topography by assembling PS colloids between two surfaces and removing the solvent used to deposit

(89) Whittle, J. D.; Barton, D.; Alexander, M. R.; Short, R. D. *Chem. Commun.* **2003**, 1766−1767.
(90) Alexander, M. R.; Whittle, J. D.; Barton, D.; Short, R. D. *J. Mater. Chem.* **2004**, *14*, 408−412.
(91) Parry, K. L.; Shard, A. G.; Short, R. D.; White, R. G.; Whittle, J. D.; Wright, A. *Surf. Interface Anal.* **2006**, *38*, 1497−1504.
(92) Xu, C.; Wu, T.; Mei, Y.; Drain, C. M.; Batteas, J. D.; Beers, K. L. *Langmuir* **2005**, *21*, 11136−11140.
(93) Xu, C.; Barnes, S. E.; Wu, T.; Fischer, D. A.; DeLongchamp, D. M.; Batteas, J. D.; Beers, K. L. *Adv. Mater.* **2006**, *18*, 1427−1430.
(94) Tomlinson, M. R.; Genzer, J. *Chem. Commun.* **2003**, No. 12, 1350−1351.
(95) Tomlinson, M. R.; Genzer, J. *Langmuir* **2005**, *21*, 11552−11555.
(96) Tomlinson, M. R.; Efimenko, K.; Genzer, J. *Macromolecules* **2007**, *39*, 9049−9056.
(97) Domingo, A. *Anal. Biochem.* **1990**, *190*, 88−90.
(98) Shearer, Jr., G. *Anal. Biochem.* **1994**, *221*, 397−400.
(99) Ogawa, K.; Kokufuta, E. *Langmuir* **2002**, *18*, 5661−5667.
(100) May, E. L.; Hillier, A. C. *Anal. Chem.* **2005**, *21*, 6487−6493.
(101) Jayaraman, S.; May, E. L.; Hillier, A. C. *Langmuir* **2006**, *22*, 10322−10328.
(102) Dobashi, T.; Nobe, M.; Yoshihara, H.; Yamamoto, T.; Cono, A. *Langmuir* **2004**, *20*, 6530−6534.
(103) Pelham, R. J., Jr.; Wang, Y.-L. *Proc. Natl. Acad. Sci. U.S.A.* **1997**, *94*, 13661−13665.
(104) Lo, C.-M.; Wang, H.-B.; Dembo, M.; Wang, Y.-l. *Biophys. J.* **2000**, *79*, 144−152.
(105) Wong, J. Y.; Velasco, A.; Rajagopalan, P.; Pham, Q. *Langmuir* **2003**, *19*, 1908−1913.
(106) Zaari, N.; Rajagopalan, P.; Kim, S. K.; Engler, A. J.; Wong, J. Y. *Adv. Mater.* **2004**, *16*, 2133−2137.
(107) Einaga, Y.; Kim, G.-S.; Ohnishi, K.; Soo-Gil Park, S.-G.; Fujishima, A. *Mater. Sci. Eng. B* **2001**, *83*, 19−23.
(108) Tsai, I. Y.; Kimura, M.; Russell, T. P. *Langmuir* **2004**, *20*, 5952−5957.
(109) Mansky, P.; Huang, E.; Liu, Y.; Russell, T. P.; Hawker, C. *Science* **1997**, *275*, 1458−1460.
(110) Erbil, H. Y.; Demirel, A. L.; Avci, Y. *Science* **2003**, *299*, 1377−1380.
(111) Lu, X.; Zhang, J.; Zhang, C.; Han, Y. *Macromol. Rapid Commun.* **2005**, *26*, 637−642.
(112) Zhang, J.; Xue, L.; Han, Y. *Langmuir* **2005**, *21*, 5−8.

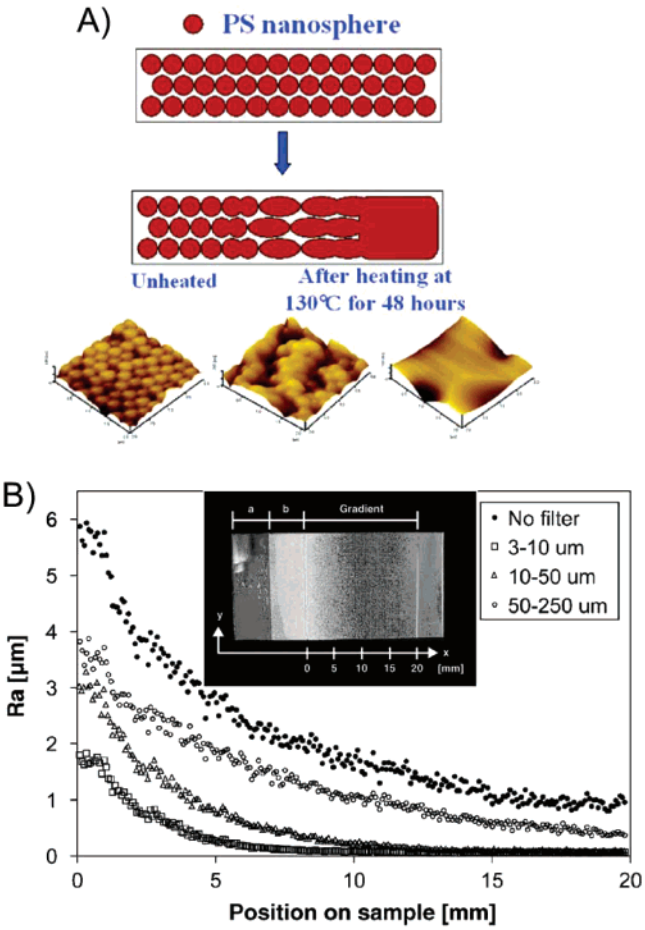

Figure 3. (A) Fabrication of substrates exhibiting a gradient in surface roughness by gradually heating polystyrene nanospheres deposited on the substrate resulting in gradient surfaces by changing polystyrene microsphere topography. AFM images at different locations of the film ranging from the unheated side to the annealed (∼130 °C) side of the substrate[112] (reproduced with permission from the American Chemical Society). (B, Inset) Photograph of a roughness gradient on an aluminum surface over a distance of 20 mm. Roughness values R_a are calculated for different wavelength windows (main figure). Data was acquired on an aluminum roughness gradient by optical profilometry and evaluated by applying fast Fourier transformation[115] (reproduced with permission from Elsevier).

the PS beads[113] or by gradually forming a density gradient of colloidal spheres on surfaces by the vertical deposition method based on graded concentration suspension.[114] Kunzler and co-workers reported recently on fabricating roughness gradients using a two-step process[115] that involved roughening alumina substrates with sand blasting by means of fractured corundum particles followed by gradually polishing the rough substrate by immersing the sample vertically into a solution consisting of a mixture of phosphoric, sulfuric, and nitric acids at elevated temperatures (Figure 3B). They used such substrates as masters for replicating the gradually changing topography into various polymer-based materials. Huwiler and co-workers generated corrugated substrates with gradients in topography by gradually dip coating silicon wafers treated with poly(ethylene amine) into colloidal suspensions of negatively charge silica particles, thus producing density gradient of nanoparticles on flat substrates. The final sample finish was achieved by sintering the substrate at elevated temperatures (>1000 °C).[116] Such substrates were then used to investigate the effect of substrate topography on cell adhesion.[117,118]

2. Gradient Dimensionality

Gradients on surfaces can exist in various dimensions; the dimensionality of a gradient structure is derived primarily from the dimensionality of the matrix onto (into) which the gradients are deposited. Although to the best of our knowledge no example of a true 1D gradient on a rod/wire has been reported, several 1D gradient structures have been fabricated on flat substrates and will be discussed below. Two-dimensional gradients can be formed by combining some of the aforementioned techniques of preparing gradients, say chemical, and using them as templates for further processing. Protein adsorption or cell adhesion fall into this category and will be discussed in more detail in section 6, where we describe selected examples pertaining to gradient functionality. As we will discuss later in this section, 2D chemical gradients represent a suitable platform for producing 3D gradient arrangements.

Early work pertaining to creating 3D gradients involved the deposition of polymer films using the "knife-edge coating" method,[85−88] which enabled the formation of polymer-based structures with gradual variations in composition and thickness. Although easy to apply to just about any type of surface, this procedure typically leads to only a physisorbed layer of polymer film on a solid support. To graft polymer films chemically to the substrate in a 3D manner, one can apply some variant of either "grafting-onto" or "grafting-from" techniques.[119] In grafting-onto coatings, preformed polymer chains are simply attached to a given surface via chemical reaction between functional groups present on the surface and those along polymer chains (typically attached to the end of the macromolecule). In contrast, grafting-from methods involve polymerization from surface-bound polymerization initiator centers chemisorbed on the substrate. Both methodologies have their advantages and disadvantages; these have been disclosed in full detail elsewhere and will not be discussed here.[119]

Polymer gradients based on grafting-onto method have been pioneered by Luzinov, Minko, and co-workers. They prepared a gradient in grafting density (i.e., number polymer chains per unit area) of polymer chains by first priming the substrate with sticky groups, such as 3-glycidoxypropyl trimethoxysilane (GPS) or poly(glycidyl methacrylate) (PGMA), spin coating an end-functionalized polymer onto such a substrate, and placing the assembly onto a heating stage with a temperature gradient (Figure 4A). After annealing, the nongrafted polymer chains were simply washed off of the specimen.[120] This method can also be conveniently used to generate 3D structures comprising a gradual variation of grafting densities of two polymers.[121,122] Here a gradient of the first polymer is formed as described previously. This step is followed by grafting a second end-functionalized polymer on top of the existing gradient structure. Ionov and

(113) Zhang, J.; Xue, L.; Han, Y. *Langmuir* **2005**, *21*, 5667−5671.
(114) Li, J.; Han, Y. *Langmuir* **2006**, *22*, 1885−1890.
(115) Kunzler, T. P.; Drobek, T.; Sprecher, C. M.; Schuler, M.; Spencer, N. D. *Appl. Surf. Sci.* **2006**, *253*, 2148−2153.
(116) Huwiler, C.; Kunzler, T. P.; Textor, M.; Vörös, J.; Spencer, N. D. *Langmuir* **2007**, *23*, 5929−5935.
(117) Kunzler, T. P.; Drobek, T.; Schuler, M.; Spencer, N. D. *Biomaterials* **2007**, *28*, 2175−2182.
(118) Kunzler, T. P.; Huwiler, C.; Drobek, T.; Vörös, J.; Spencer, N. D. *Biomaterials* **2007**, *33*, 5000−5006.
(119) *Polymer Brushes*; Brittain, B., Advincula, R., Rühe, J., Caster, K., Eds.; Wiley & Sons: New York, 2004.
(120) Ionov, L.; Zdyrko, B.; Sidorenko, A.; Minko, S.; Klep, V.; Luzinov, I.; Stamm, M. *Macromol. Rapid. Commun.* **2004**, *25*, 360−365.
(121) Ionov, L.; Sidorenko, A.; Stamm, M.; Minko, S.; Zdyrko, B.; Klep, V.; Luzinov, I. *Macromolecules* **2004**, *37*, 7421−7423.
(122) Ionov, L.; Sidorenko, A.; Eichhorn, K.-J.; Stamm, M.; Minko, S.; Hinrichs, K. *Langmuir* **2005**, *21*, 8711−8716.

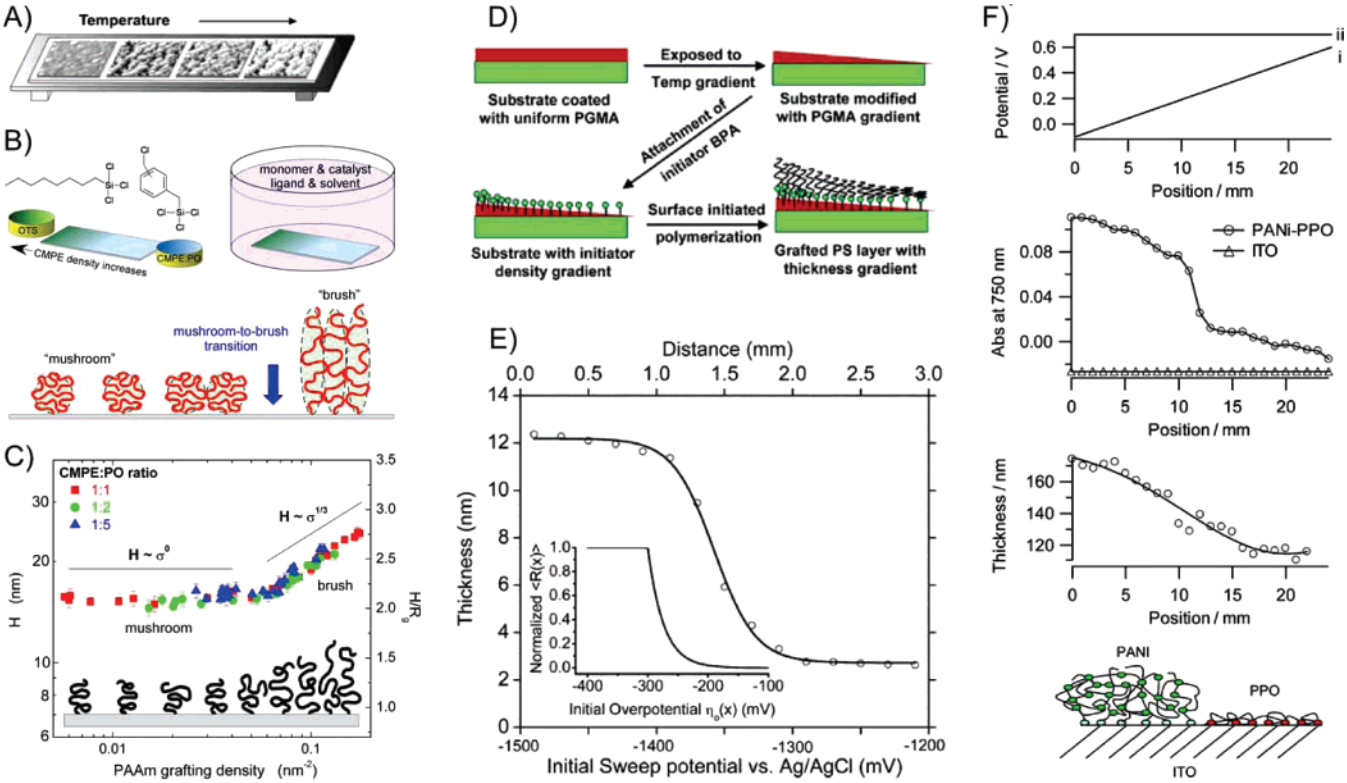

Figure 4. (A) Preparation of ultrathin tethered polymer layers with gradually changing thickness by combining a grafting-onto method with a temperature gradient created on a heating stage[120] (reproduced with permission from Wiley). (B) Method of preparing surface-anchored polymer assemblies with gradients in grafting density by first creating a molecular gradient of 1-trichlorosilyl-2-(*m*/*p*-chloromethylphenyl) ethane (CMPE) initiator diluted to different ratios with paraffin oil (PO), followed by grafting-from polymerization of poly(acryl amide) (PAAm). (C) Wet thickness of PAAm brushes as a function of the PAAm grafting density. The samples were prepared on substrates containing the initiator gradients made from 1:1 (squares), 1:2 (circles), and 1:5 (triangles) CMPE/PO mixtures (w/w)[126] (reproduced with permission from the American Chemical Society). (D) Synthesis of high-density grafted polymer layers with thickness and grafting density gradients[134] (reproduced with permission from the American Chemical Society). (E) Thickness of a poly(acrylic acid) gradient formed by a dynamic potential gradient (DPG) method. The inset shows the form of the DPG thickness gradient[136] (reproduced with permission from the American Chemical Society). (F) Formation of a poly(aniline) (PANI) and poly(phenylen oxide) (PPO) two-band sample on indium tin oxide (ITO). (Top to Bottom) Potential profiles used to create polymer bands: (i) $E_1 = -0.1$ V and $E_2 = 0.6$ V in phenol solution and (ii) $E_1 = E_2 = 0.7$ V in aniline solution. Optical absorbance at 750 nm measured at various positions along the sample for bare ITO and ITO with a PANI-PPO film. Thickness of a PANI-PPO film as measured by null ellipsometry. Schematic of the ITO substrate with polymer films[138] (reproduced with permission from the American Chemical Society).

co-workers later extended the same procedure to the preparation of gradients of PEG films on PGMA-coated silica surfaces and used it to form gradients of kinesin motor molecules.[123] Another method involving the grafting-onto technique leading to grafting density gradients of macromolecules was developed by Mougin and co-workers.[124] In their technique, a gold-coated substrate was first covered with a SAM of cystamine, which introduced amino groups onto the surface. After the substrate was covered with an ~1 mm layer of agarose gel, a small capillary was inserted vertically into the substrate though which a solution of *N*-hydroxysuccinimide ester (NHS)-terminated PEG was delivered. As it traveled across the surface, the PEG-NHS was immobilized on the surface by reacting with the primary amine groups on the surface. This method was closely related to that presented earlier by Halfter, who reported on forming radial gradients of basal lamina proteins in a drop of Hank's solution residing on a white membrane filter by means of a capillary inserted into the Hank's solution phase.[125]

Most recent efforts included decorating the substrate with polymer brush assemblies comprising a gradual variation of grafting density,[126−129] thickness (i.e., polymer length),[130] and polymer composition.[94−96] Our group has made a few important contributions here. Specifically, Wu and co-workers reported on the fabrication of polymer grafting density gradients on flat silica-based surfaces (Figure 4B,C). In their method, a gradient of organosilane-based initiator for atom-transfer radical polymerization (ATRP) was generated by the vapor diffusion method,[34] followed by backfilling the substrate with a hydrophobic organosilane SAM. Wu et al. also demonstrated the feasibility of reversing the process, namely, forming a molecular gradient of the hydrophobic "filler" followed by filling the empty surface sites with an ATRP-based initiator. Grafting-from polymerization then commenced from the surface-anchored initiating centers. Such gradient assemblies were formed from a large variety of polymers. Zhao extended the earlier work of Wu and co-workers

(123) Ionov, L.; Stamm, M.; Diez, S. *Nano Lett.* **2005**, *5*, 1910−1914.
(124) Mougin, K.; Ham, A. S.; Lawrence, M. B.; Fernandez, E. J.; Hillier, A. C. *Langmuir* **2005**, *21*, 4809−4812.
(125) Halfter, W. *J. Neurosci.* **1996**, *16*, 4390−4401.
(126) Wu, T.; Efimenko, K.; Genzer, J. *J. Am. Chem. Soc.* **2002**, *124*, 9394−9395.
(127) Wu, T.; Efimenko, K.; Vlèek, P.; Šubr, V.; Genzer, J. *Macromolecules* **2003**, *36*, 2448−2453.
(128) Wu, T.; Genzer, J.; Gong, P.; Szleifer, I.; Vlèek, P.; Šubr, V.; Behavior of Surface-Anchored Poly(acrylic acid) Brushes with Grafting Density Gradients on Solid Substrates. In *Polymer Brushes*; Brittain, B., Advincula, R., Rühe, J., Caster, K., Eds.; Wiley & Sons: New York, 2004; Chapter 15, p 287.
(129) Wu, T.; Gong, P.; Szleifer, I.; Vlček, P.; Šubr, V.; Genzer, J. *Macromolecules* **2007**, *40*, 8756−8764.
(130) Tomlinson, M. R.; Genzer, J. *Macromolecules* **2003**, *36*, 3449−3451.

by developing a method for fabricating "double" grafting density gradients of two chemically distinct polymers propagating in two opposite directions on the substrate.[131] In this method, a gradient of ATRP-based initiator was formed by the vapor deposition method,[34] followed by backfilling the substrate empty sites with initiator molecules for nitroxide-mediated radical polymerization (NMRP). PMMA and PS brushes were then synthesized by sequential grafting-from polymerization using the ATRP and NMRP initiator centers, respectively, resulting in PS and PMMA brush grafting density gradients counter-propagating in two opposite directions. Wang and Bohn developed a complementary method for generating double gradients of grafted polymers by utilizing the electrochemical deposition of ATRP initiator followed by grafting-from polymerization of *N*-isopropyl acrylamide (NIPAAm). In the subsequent step, additional ATRP initiator was electrochemically inserted into the "empty" spaces on the gold-covered substrate; these served as initiating sites for the ATRP of 2-hydroxyethyl methacrylate (HEMA).[132] Wang and co-workers also prepared density gradients of ATRP initiator by electrochemical means and performed grafting-from polymerization of NIPAAm using ATRP.[133] An elegant way of controlling the grafting density of macromolecules on surfaces was developed by Luzinov and co-workers (Figure 4D).[134] Capitalizing on their earlier work with PGMA, the researchers formed a gradient of PGMA on the surface followed by attachment of 2-bromo-2-methylpropionic acid (BPA) onto the PGMA-grafted substrate. Subsequent ATRP-based polymerization of styrene from the surface-anchored BPA centers produced PS brushes with very high grafting densities (0.75−1.5 chains/nm^2).

Thickness gradients of polymer brushes on substrates were formed by several methods. We have reported on two such techniques. Tomlinson and co-workers first utilized a technique in which a flat substrate previously decorated with initiator molecules was placed vertically into a glass chamber, which was filled with the polymerization mixture (monomer, catalyst, and solvent).[130] A micropump attached to the bottom of this chamber gradually drained the chamber of the polymerization medium, thus slowly lowering the level of the solution along the substrate. Because the length of the grown polymer was directly proportional to the time for which the substrate was in contact with the polymerization medium, the top of the substrate contained short polymers (shorter contact time with the polymerization medium), and the bottom of the substrate was covered with polymers having a higher molecular weight (longer contact time with the polymerization medium). Tomlinson and co-workers later reported on another method of producing molecular weight gradients of surface-tethered polymers. Here, instead of removing the polymerization medium, the sample was vertically lowered into the solution using a custom-designed dipping apparatus.[96] Alternative methods leading to the formation of polymer assemblies with gradients in chain length have been developed by other groups. For instance, Xu and co-workers developed an analog to the aforementioned draining method for preparing surface-bound polymer gradients by placing a silicon wafer covered with polymerization initiator vertically into a chamber and filled the chamber from the bottom with polymerization media.[135] Wang and Bohn reported on preparing gradients of poly(acrylic acid) (PAA) by the Zn(II)-catalyzed electropolymerization of acrylic acid in the presence of an in-plane electrochemical potential gradient applied to Au electrodes (Figure 4E).[136] In subsequent work, they reported on derivatizing the PAA matrix with fluorocarbons and RGD-containing peptides and prepared PNIPAAm brushes, which were doped with gold nanoparticles.[137] Ratcliff and Hillier deposited polymers onto substrates using spatially controllable electric field gradients (Figure 4F).[138] In addition to the conventional field-free methods and electroassisted deposition, photopolymerization technologies have also been utilized to generate gradient polymer-based assemblies.[139] Khire and co-workers reported on using surface-initiated thiol-ene photopolymerization.[140] They tailored the properties of the surface-bound polymer by varying the density of the initiator on the surface (grafting density gradient) and/or the photopolymerization conditions (molecular weight gradient). A thiol-acrylate Michael-type reaction was used to dope the resulting polymer gradients with Arg-Gly-Asp-Ser (RGDS) cell-adhesive peptide, which yielded a gradient in osteoblast density on the surface. Harris and co-workers reported independently on creating polymer gradient assemblies using substrate-induced photopolymerization of poly(methacrylic acid),[141] which was used as a support for RGD-based peptides, thus creating ligand density gradients for the position-dependent adhesion of fibroblast cells.[142] Three-dimensional polymer assemblies with gradients in grafting density and molecular weight enabled the systematic investigation of the behavior of weak polyelectrolyes,[128,129] nanoparticle dispersion,[137,143−147] protein adsorption, cell adhesion, and others discussed in more detail in section 6 of this article.

A gradual variation of chemistry in the vertical direction has been achieved with random copolymer brushes as described by Xu and co-workers.[92] They formed surface-anchored gradient random copolymers on flat substrates comprising MMA and HEMA monomers by polymerizing MMA on a vertically standing silicon wafer covered with surface-anchored initiator and steadily adding HEMA to the reaction mixture. As a result, the copolymer was MMA-rich in the initial stages and HEMA-rich in the final stages of polymerization. Xu and co-workers also developed an alternative approach for generating such surface-grafted statistical copolymer assemblies. Specifically, they used a microfluidic mixer to mix solutions of two different monomers with different volumetric flows and fed the monomer mixture into the bottom of a polymerization chamber, where a silicon substrate covered with initiator molecules was placed vertically. In this manner, the chamber was filled from the bottom to the top, thus producing random copolymer with a gradient in composition.[93] Gradients comprising block copolymers with ordered sequence distributions have also been realized by repeating the draining, dipping, or filling procedure described above with two different mono-

(131) Zhao, B. *Langmuir* **2004**, *20*, 11748−11755.
(132) Wang, X.; Bohn, P. W. *Adv. Mater.* **2007**, *19*, 515−520.
(133) Wang, X.; Tu, H.; Braun, P. V.; Bohn, P. W. *Langmuir* **2006**, *22*, 817−823.
(134) Liu, Y.; Klep, V.; Zdyrko, B.; Luzinov, I. *Langmuir* **2005**, *21*, 11806−11813.
(135) Xu, C.; Wu, T.; Batteas, J. D.; Drain C. M.; Beers, K. L.; Fasolka, M. J. *Appl. Surf. Sci.* **2005**, *252*, 2529−2534.
(136) Wang, X.; Bohn, P. W. *J. Am. Chem. Soc.* **2004**, *126*, 6825−6832.
(137) Wang, X.; Haasch, R. T.; Bohn, P. W. *Langmuir* **2005**, *21*, 8452−8459.
(138) Ratcliff, E.; Hillier, A. C. *Langmuir* **2007**, *23*, 9905−9910.
(139) Higashi, J.; Nakayama, Y.; Marchant, R. E.; Matsuda, T. *Langmuir* **1999**, *15*, 2080−2088.
(140) Khire, V. S.; Benoit, D. W. S.; Anseth, K. S.; Bowman, C. N. *J. Polym. Sci.: Polym. Chem. A* **2006**, *44*, 7027−7039.
(141) Harris, B. P.; Metters, A. T. *Macromolecules* **2006**, *39*, 2764−2772.
(142) Harris, B. P.; Kutty, J. K.; Fritz, E. W.; Webb, C. K.; Burg, K. J. L.; Metters, A. T. *Langmuir* **2006**, *22*, 4467−4471.
(143) Bhat, R. R.; Genzer, J.; Chaney, B. N.; Sugg, H. W.; Liebmann-Vinson, A. *Nanotechnology* **2003**, *14*, 1145−1152.
(144) Bhat, R. R.; Tomlinson, M. R.; Genzer, J. *Macromol. Rapid Commun.* **2004**, *25*, 270−274.
(145) Bhat, R. R.; Genzer, J. *Appl. Surf. Sci.* **2005**, *252*, 2549−2554.
(146) Bhat, R. R.; Genzer, J. *Surf. Sci.* **2005**, *596*, 187−196.
(147) Bhat, R. R.; Genzer, J. *Nanotechnology* **2007**, *18*, 025301-1−025301-6.

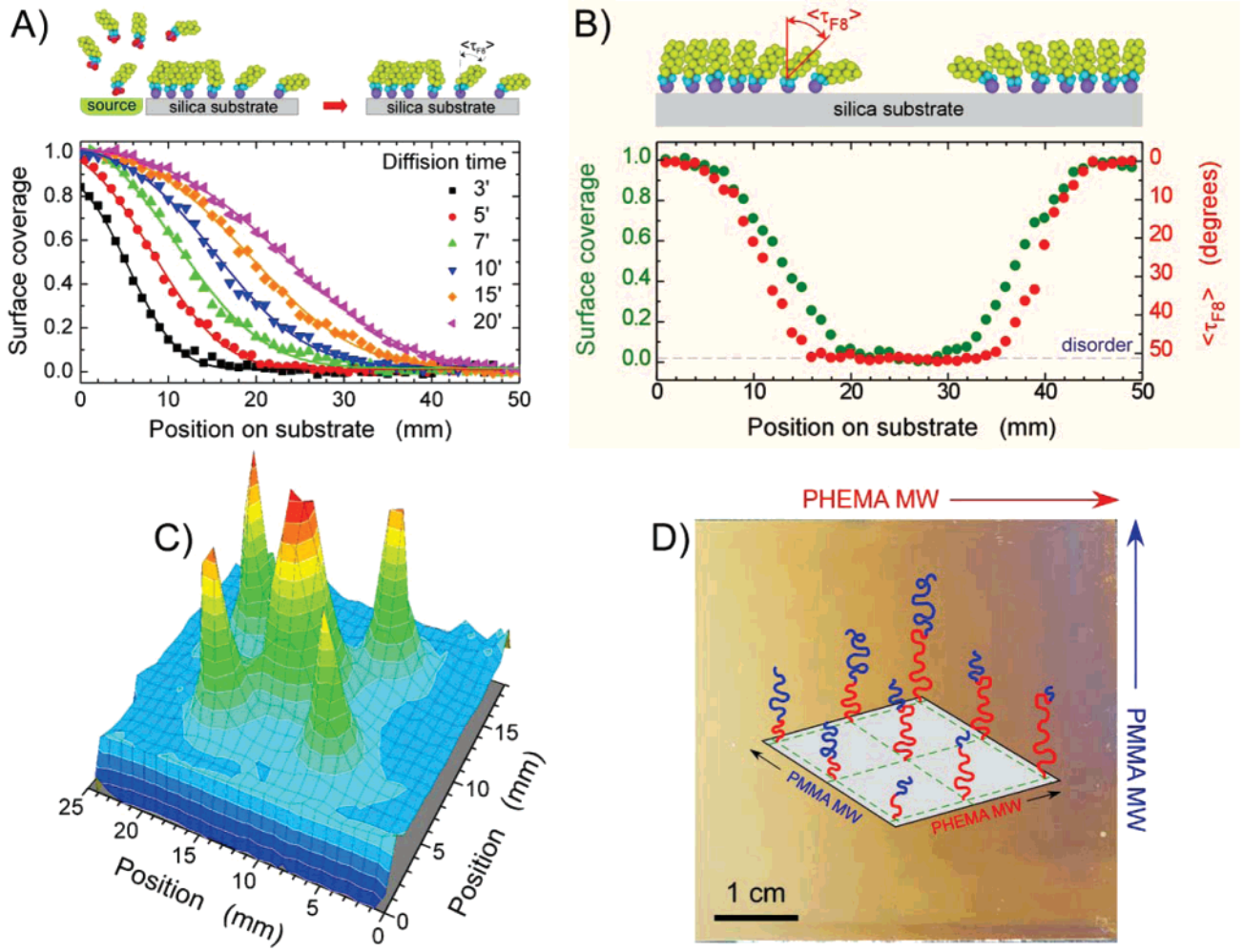

Figure 5. Examples of directional gradients. (A) Frontal spreading of a monoalkoxyfluorine-terminated silane (1H,1H,2H,2H-perfluorodecyldimethylchlorosilane, mF8H2) as a function of time on a silica substrate. The organosilane layers are formed as indicated in the schematic, and the surface coverage refers to the silane concentration relative to the fully ordered layer[206] (reproduced with permission from the National Academy of Sciences). (B) Fraction of 1H,1H,2H,2H-perfluorodecyltrichlorosilane (tF8H2) in the SAM (f_{F8H2}) (green circles) and the average surface orientation (red circles) of tF8H2 molecules ($\langle\tau_{F8}\rangle$) in the double gradient as a function of the position on the substrate[5] (reproduced with permission from the American Institute of Physics). (C) Silane concentration maps determined by combinational NEXAFS from radial gradients of tF8H2 prepared by depositing small droplets of the silane and letting them evaporate for 1 min (Genzer, J.; Efimenko, K., unpublished results). (D) Photograph of an orthogonal polymer gradient comprising surface-anchored diblock copolymers made of poly(2-hydroxy methacrylate) and poly(methyl methacrylate) blocks with variable lengths of both blocks. The gradual color variation along the two axes of the photograph is due to the variation in the total thickness of the copolymer (Tomlinson, M. R.; Genzer, J., unpublished results). A schematic drawn in the center of the photograph depicts the design of the orthogonal gradient.

mers.[92−96] We will describe one such technique in more detail in section 3, discussing gradient directionality.

The previous examples discussed the preparation of 3D gradients that were bound to a substrate. In addition, methods have been developed that facilitate the formation of 3D gradients in "true 3D space". An example of such effort is a study by Rosoff and co-workers who prepared molecular gradients in gels.[148] The gradient patterns were produced by pumping liquids at adjusted volumetric flows into a collagen gel while moving the gel "substrate" via a translation stage. Other examples mentioned earlier involve 3D gradients of pH[99] and refractive index.[102]

3. Gradient Directionality

All gradients are, by definition, directional; the properties of substrates covered by gradients change gradually in a particular direction across the substrate. The most widely used gradient assemblies are those that possess a variation of some physicochemical property in one direction. We coin such a gradient as directional or unidirectional (Figure 5A). Even for unidirectional gradients, one can fabricate substrates on which two gradients of the same type propagate from two opposite directions and may eventually collide (Figure 5B). An obvious extension of unidirectional gradients involves so-called radial gradients in which the gradual variation of physicochemical character occurs radially on the substrate, commencing at a central point somewhere on the substrate. Radial gradients combining multiple "gradient satellites" can also be designed. Here the individual gradients may remain isolated or can combine, as illustrated by the wettability gradient arising from five diffusion sources (Figure 5C).

Although the gradients mentioned above involve the variation of a single property (say, chemistry), one can readily extend the same concept to gradients involving a gradual variation of more than one characteristic. Unidirectional gradients comprising, for instance, a gradual variation of roughness in one direction and

(148) Rosoff, W. J.; McAllister, R.; Goodhill, G. J.; Urbach, J. S. *Biotechnol. Bioeng.* **2005**, *91*, 754−759.

a gradual change in chemical composition in the opposite direction are examples of such structures. One special class of multigradient substrates involves an orthogonal gradient motif, wherein two properties vary independently across the specimen in two mutually perpendicular directions. These gradients can involve a change in two different chemistries or can be made of two dissimilar characteristics, say, chemistry and roughness or chemistry and substrate rigidity (i.e., modulus). Meredith and co-workers pioneered methods enabling the preparation of orthogonal gradients exhibiting variations of (1) polymer film thickness/chemical composition,[85] (2) film chemical composition/process temperature,[85] and (3) polymer film thickness/temperature.[86] These structures facilitated a systematic, fast screening of phase behavior in two-component polymer mixtures (i.e., generating continuous phase diagrams) and probing thin film stability (i.e., dewetting) on solid impenetrable supports.

Our group published a series of papers illustrating various methods leading to the formation of orthogonal polymer assemblies comprising the gradual and independent variation of (1) molecular weight and grafting density (MW−σ) and (2) the molecular weight of two blocks in a diblock copolymer (MW1−MW2). The MW−σ structures were prepared by first decorating flat substrates (i.e., silicon wafer, glass) with a molecular gradient of polymerization initiator, followed by grafting-from polymerization using the draining or dipping method, described earlier in section 2, in the direction orthogonal to that of the grafted initiators.[17,18,144,149,150] The MW1−MW2 gradients were fabricated by first preparing a length gradient of the first polymer by means of grafting-from polymerization using the draining or dipping method, rotating the sample orthogonally, and repeating the first step with another monomer.[17,18,95] In the latter case, the first polymer acted as a macroinitiator for the growth of the second block. Figure 5D illustrates an example of an orthogonal gradient composed of surface-anchored diblock copolymers in which the molecular weight (or alternatively length) or each block changes gradually along two mutually perpendicular directions on the sample. Other groups have also reported on preparing orthogonal gradients using the grafting-from method. For instance, Khire and co-workers reported on creating orthogonal grafting density−molecular weight gradients of polymers by utilizing thiol-ene photopolymerization reactions.[140]

Obviously, one can extend the concept of multidirectional gradients even further. To this end, triangular gradients can be generated that allow for the variation of three independent characteristics. Tomlinson and co-workers recently fabricated such substrates decorated with triblock copolymers comprising blocks of poly(methyl methacrylate), poly(2-hydroxyelthyl methacrylate), and poly(dimethylaminoethyl methacrylate) with a gradual variation of the lengths of the individual blocks.[151] Moreover, in switching from 2D to 3D, one can potentially think of producing tetrahedral gradients where four individual quantities vary in space gradually. To the best of our knowledge, no examples of the latter category of gradients have yet been reported.

4. Gradient Length Scale

Each gradient is characterized by an inherent length scale over which a surface physicochemical property changes gradually. To this end, each gradient can be viewed as having dual character. First, a gradual variation can be observed on the inherent gradient length scale (i.e., the length scale associated with the overall gradual variation of a given property on the substrate). In addition, on length scales significantly smaller than the inherent length scale, the structure appears to exhibit a uniform property. The overall sample can then be considered to be a collection of individual homogeneous specimens, each having a discrete property. Consequently, any array of discrete spots on the surface, where the property (say, composition) of each element of the array changes gradually, can be considered to possess the attributes of a gradient, provided the spots are positioned close enough that on the large length scale the structure appears to be nearly continuous. This dual nature (discrete on nano/microscales and continuous on the mesoscale) makes gradients a powerful tool for both systematically studying various physicochemical phenomena and driving certain phenomena.

When using gradients for materials property screening (i.e., using the gradient structures as a library of individual homogeneous specimens), it is imperative to ensure that the characteristics of the individual library elements remain constant in order to attain an acceptable uncertainty in the measured property.[88] Obviously, the actual size of the discrete spots on the sample, into which the overall gradient structure can be subdivided, depends crucially on the lateral resolution of a given technique. Thus, the sample has to be large enough and the gradient "steepness" has to be small enough so that the size of an individual element of the library possesses a uniform property. In cases where the gradient nature is to be utilized in affecting a given phenomenon (e.g., driving a motion of some adsorbed objects such as liquid drops), the gradient steepness has to be of the same order as the length scale sampled by the moving object on the substrate (i.e., characteristic contact length scale of the moving object plus a contribution associated with the object's Brownian motion on the substrate). Hence, gradients whose steepness changes over a millimeter to centimeter range are suitable for driving the motion of liquid drops. (For details, see section 6 for a discussin of gradient functionality.) However, if one intends to utilize gradient substrates to study a phenomenon, which take place on a much smaller length scale (e.g., cell migration), then the substrates have to be used that change their material characteristics on a much smaller length scale (submillimeter or even smaller).

Most gradient geometries described thus far span over a distance of a few millimeters to centimeters. There are, however, some methods that allow for considerably decreasing the spatial dimension of the gradient patterns. These involve the method of creating molecular gradients on flexible substrates (Figure 6A),[76] replacement lithography (Figure 6B),[45] deposition of organosilanes by means of silicone elastomer (SE) stamps with different curvatures (Figure 6C),[48] chemically converting alkenethiol-based SAM molecules with soft X-rays,[52,53] or edge-spreading lithography.[54] It is our hope that with the rapid development of various patterning tools capable of controlling the spatial distribution of "blueprints" on surfaces more technologies will soon be available that would permit the generation of chemical and/or physical gradients on the nanometer scale.

5. Gradient Temporal Dependency

Most gradient structures can be termed static; thus, their physicochemical properties have been fixed at the time of their creation. However, for some operations it is advantageous to create gradients that can change their properties in response to a variation of some external stimulus, such as solvent quality, pH, temperature, electric or magnetic field, ion concentration, and others.

(149) Bhat, R. R.; Genzer, J. *Mater. Res. Soc. Symp. Proc.* **2004**, *804*, JJ.5.8.1−JJ.5.8.9.

(150) Bhat, R. R.; Chaney, B. N.; Rowley, J.; Liebmann-Vinson, A.; Genzer, J. *Adv. Mater.* **2005**, *17*, 2802−2807.

(151) Tomlinson, M. R.; Genzer, J. To be submitted for publication.

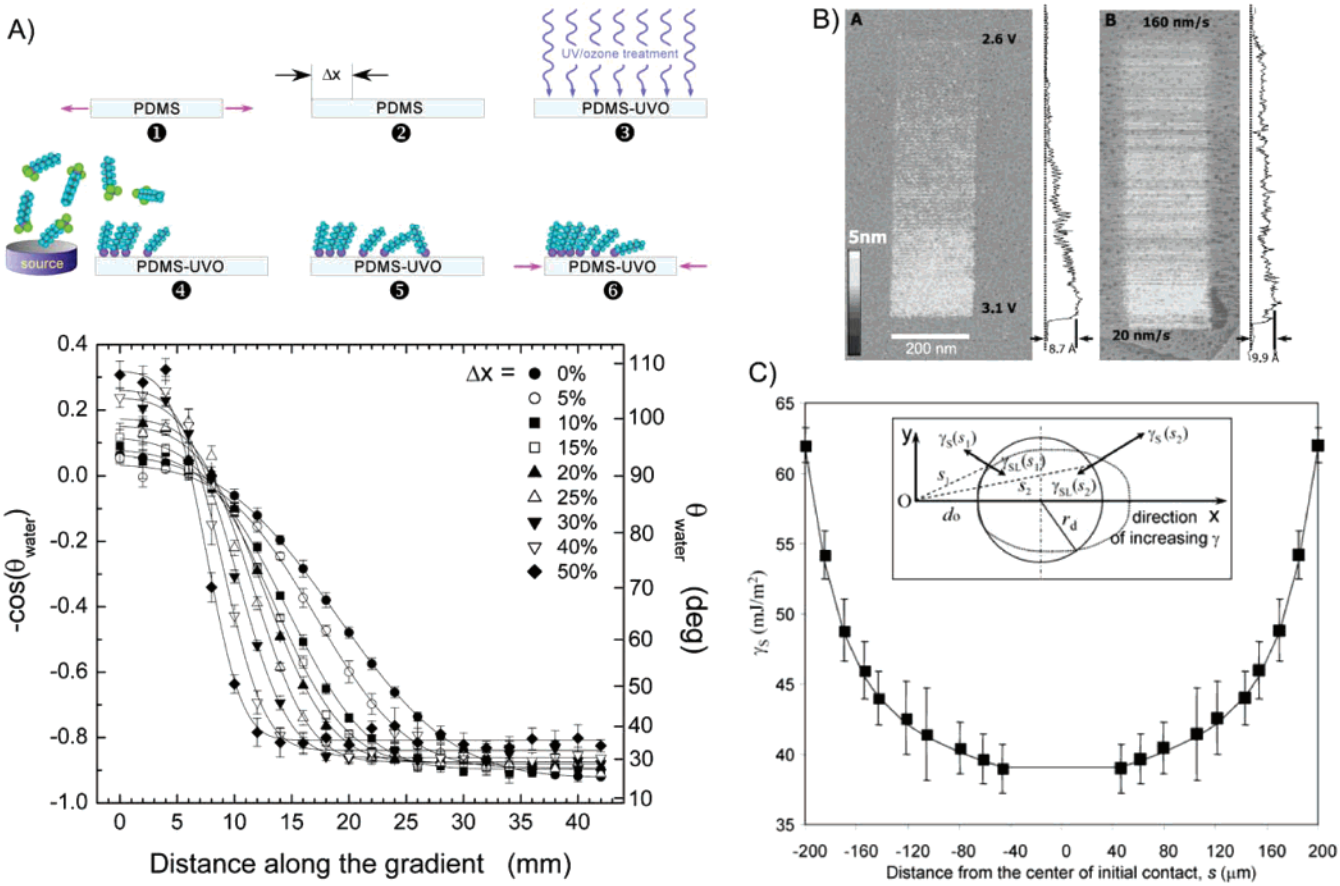

Figure 6. (A) Schematic depicting the creation of mechanically assembled monolayer (MAM) gradients. These gradients were prepared by vapor deposition of octyltrichlorosilane on stretched and UVO-treated PDMS network films. The bottom part shows contact angles of deionized water along these MAM gradient substrates for different degrees of substrate extension[76] (reproduced with permission from Wiley). (B) STM images of FcC11S-SAM mesoscale chemical gradients fabricated by replacement lithography by systematically varying the replacement bias (left), or lithographic scan rate (right), while maintaining all other STM parameters constant. The averaged section analysis is shown to the right of each gradient structure. *z* scale: 5 nm[45] (reproduced with permission from Wiley). (C) Experimentally estimated surface energies for the gradient surface prepared by the micrometer-scaled gradient method[48] (reproduced with permission from the American Chemical Society).

Dynamic grafted polymer gradients capable of varying their properties as a function of solvent quality, pH, or charge have already been reported. For instance, substrates can be decorated by two chemically distinct polymer brushes (say, brushes A and B) that have dissimilar solubilities in various solvents. Upon changing the solvent quality, either brush A or B can swell, and the other one can collapse. Alternatively, one can think of producing substrates where the density of weak polycationic and polyanionic polymers (i.e., polymers that exhibit positive and negative charges upon altering the pH of the solution) varies independently in two opposite directions. A gradient of positive or negative charge can then be produced by simply varying the pH of the solution in which the substrates are immersed. Ionov and co-workers applied the grafting-onto method[121] (section 2) to create responsive polymer surfaces[152] comprising mixed brushes made of poly(acrylic acid) (PAA) and poly(2-vinyl pyridine) (P2VP).[153] Because the density of these two polymer constituents changed gradually across the substrate in two opposite direction, such gradients responded to the variation of pH by swelling the P2VP brushes at low pH and swelling the PAA brushes at high pH (Figure 7A).

A special type of dynamic gradient includes those that are produced by mixing various liquids in an intricately designed microfluidic device. These gradients are not surface-bound; instead, the time-dependent variation of the concentration of the various liquids is achieved in a flowing liquid. Whitesides and co-workers utilized a network of multi-inlet microfluidic channels to fabricate gradients in composition in solution and gradients in topography on the surface.[78−81] A microfluidic gradient generator consisting of multiple generation branches in a poly(dimethylsiloxane) network was fabricated by rapid prototyping[154] and soft lithography.[1] Multiple solutions were infused simultaneously into the network through the inlets. As the fluid streams traveled down the network, they were repeatedly split, mixed, and recombined. After several generations of branched systems, each branch contained different proportions of the infused solutions. A gradient was established, perpendicular to the flow, in a single large channel that combined all branches. Using this methodology, a number of gradients has been reported to date, including those of laminin and bovine serum albumin,[81] avidin, and others.[84,155] As demonstrated by Jiang and co-workers, the utilization of gradients in avidin opens up new possibilities of forming biomolecular gradients on a large variety of surfaces by

(152) *Responsive Polymer Materials: Design and Applications*; Minko, S.; Ed.; Blackwell Publishing: Ames, IA, 2006.
(153) Ionov, L.; Houbenov, N.; Sidorenko, A.; Stamm, M.; Luzinov, I.; Minko, S. *Langmuir* **2004**; *20*, 9916−9919.
(154) Duffy, D. C.; McDonald, J. C.; Schueller, O. J. A.; Whitesides, G. M. *Anal. Chem.* **1998**, *70*, 4974−4984.
(155) Paliwal, S.; Iglesias, P. A.; Campbell, K.; Hilioti, Z.; Groisman, A.; Levchenko, A. *Nature* **2007**, *446*, 46−51.

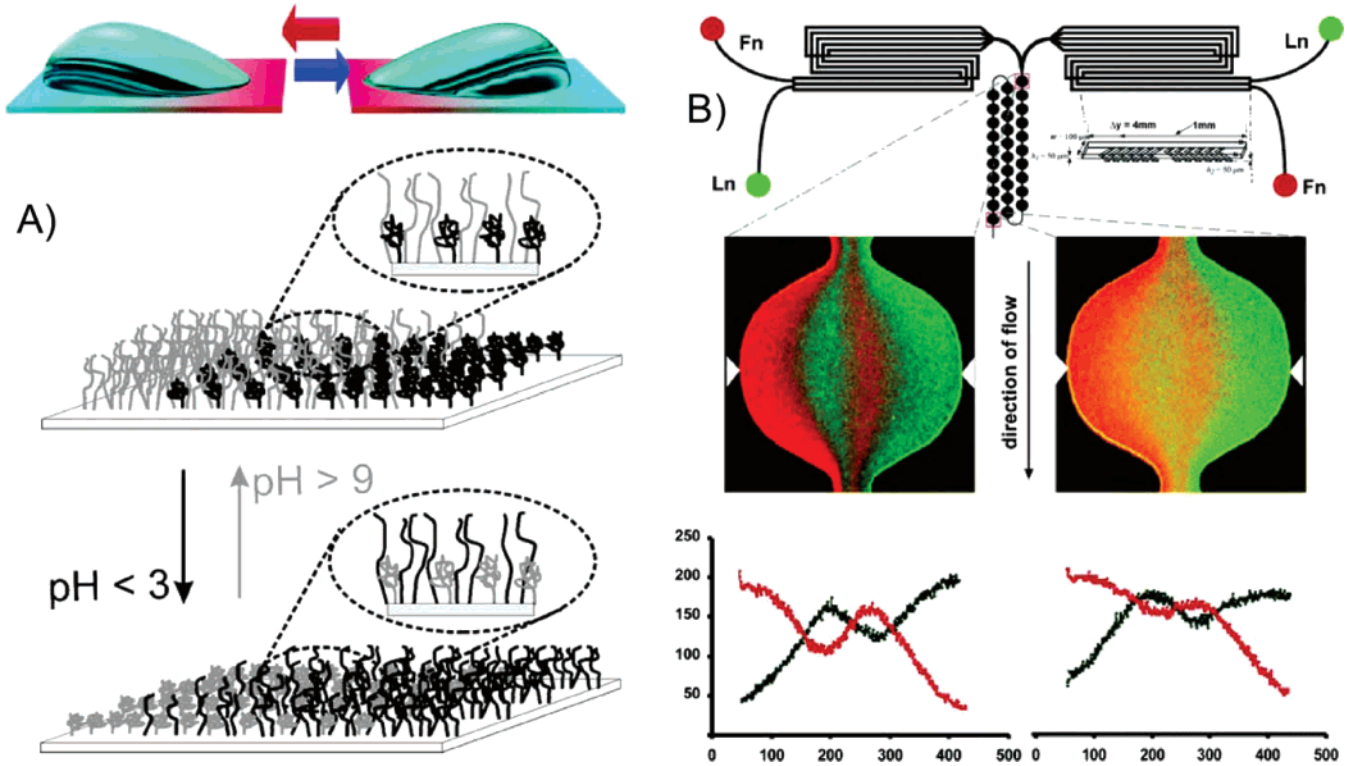

Figure 7. (A) Inverse and reversible switching of the gradient surfaces created from mixed polyelectrolyte brushes. Switching behavior of the mixed polyelectrolyte brushes of poly(acrylic acid) and poly(2-vinyl pyridine) is achieved upon changing the pH of the solution in which the substrate was immersed[153] (reproduced with permission from the American Chemical Society). (B) Combination of overlapping gradients of laminin (Ln) and fibronectin (Fn) into complex contours. (Top) Design of the microfluidic network (μFN). (Middle) Anti-Fn (mouse) and anti-Ln (rabbit) were used as primary antibodies, and anti-mouse-fluorescein and anti-rabbit-Texas red were used as secondary antibodies to visualize these gradients. Arrowheads point to the axis along which the fluorescence intensity was read (bottom panel). Fluorescence intensities as a function of the distance across the channel[84] (reproduced with permission from the American Chemical Society).

immobilizing avidin molecules on the surface and utilizing the well-known binding between avidin and biotin-containing molecules, including small molecules, DNA, proteins, and polysaccharides (Figure 7B).[84] Gunawan and co-workers used gradients of extracellular matrix proteins (laminin and collagen I) created in microfluidic networks to demonstrate control over the expression levels of two proteins linked to cell cycle progression by virtue of the spatial location of cells on the gradients.[156,157] A microfluidic setup was recently used to vary the pH of solution gradually, which enabled a dynamic nonequilibrium study of the self-assembly of collagen molecules.[158]

A few exotic types of gradients were created by varying external fields, such as temperature,[159−162] pH,[99,163] and electrochemical potential. For example, Yamada and Tada developed dynamic wettability gradients by decorating substrates with ferrocenyl alkanethiols and applying in-plane gradients in the electrochemical potential between the ends of the substrate. Reversibility in the motion of nitrobenzene and dichloromethane drops on these wettability gradients was also reported.[157,164]

6. Gradient Functionality

By their very nature, gradients are functional structures. Chemical gradients transport materials in a directional manner; they are responsible for driving many important biological and physical processes. For instance, the growth of axons from ganglions to target tissues and the directed movement of certain bacteria toward nutrients occur in response to the concentration gradients of molecules emanating from an axon target or food source.[73,74,165] Another example of active transport systems involves the locomotion of motor proteins (i.e., kinesin), which can haul cargoes attached to them along microtubular "railroads".[166] Concentration gradients of molecules in fluids or on surfaces also affect phenomena such as osmotic swelling, surface pressure, and surface wettability. The methods of forming gradients on surfaces can be applied to record some important physical phenomena. For instance, by continuously immersing a flat substrate into a polymer solution, one can systematically study the adsorption of polymers onto that substrate. Another example, discussed below, involves a study of polymerization kinetics. Substrates decorated with polymerization initiators can be slowly dipped into a solution of a monomer (and a catalyst), thus producing a gradient in the chain length of the surface-bound polymer. Measuring the chain length of such polymers grown at various points along the gradient can reveal information

(156) Gunawan, R. C.; Choban, E. R.; Concour, J. E.; Silverstre, J.; Schook, L. B.; Gaskins, H. R.; Leckband, D. E.; Kenis, P. J. A. *Langmuir* **2005**, *21*, 3061−3068.
(157) Gunawan, R. C.; Silvestre, J.; Gaskins, H. R.; Kenis, P. J. A.; Leckband, D. E. *Langmuir* **2006**, *22*, 4250−4258.
(158) Köster, S.; Leach, J. B.; Struth, B.; Pfohl, T.; Wong, J. Y. *Langmuir* **2007**, *23*, 357−359.
(159) Brochard, F. *Langmuir* **1989**, *5*, 432−438.
(160) Brzoska, J. B.; Brochard-Wyart, F.; Rondelez, F. *Langmuir* **1993**, *9*, 2220−2224.
(161) Schneemilch, M.; Cazabat, A. M. *Langmuir* **2000**, *16*, 8796−8801.
(162) Schneemilch, M.; Cazabat, A. M. *Langmuir* **2000**, *16*, 9850−9856.
(163) Phayre, A. N.; Vanegas Farfano, H. M.; Hayes, M. A. *Langmuir* **2002**, *18*, 6499−6503.
(164) Yamada, R.; Tada, H. *Langmuir* **2005**, *21*, 4254−4256.
(165) Harris, A. *Exp. Cell. Res.* **1973**, *77*, 285−297.
(166) Limberis, L.; Stewart, R. J. *Nanotechnology* **2000**, *11*, 47−51.

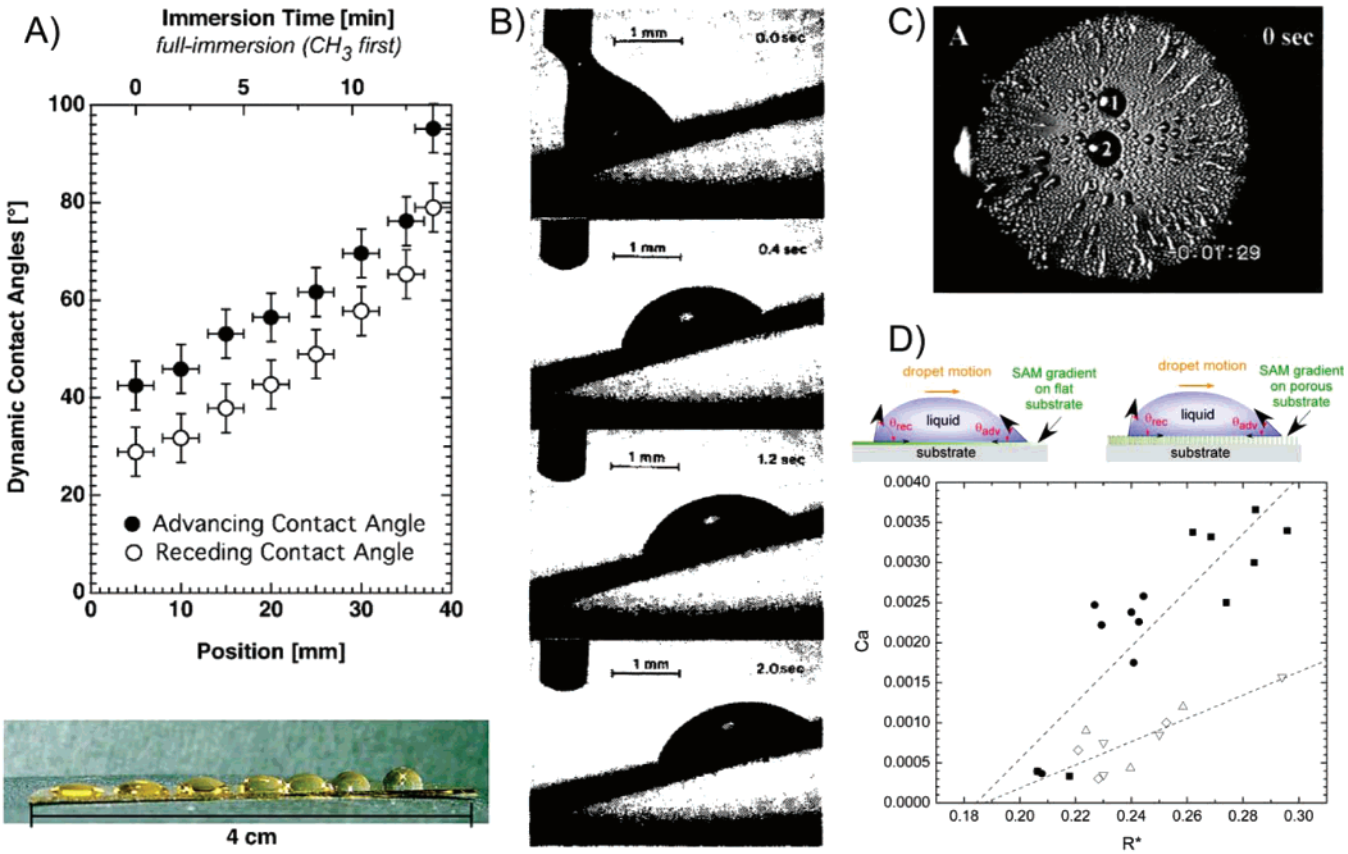

Figure 8. (A, Top) Dynamic contact angles along a hydrophobicity gradient using full-immersion (CH_3-first) as the preparation method. The small hysteresis of less than 15° between the advancing and the receding contact angles is an indication of the formation of a full monolayer. (Bottom) Water droplets along a hydrophobicity gradient using full-immersion (CH_3-first) as the preparation method[46] (reproduced with permission from the American Chemical Society). (B) Uphill motion of a drop of water (volume 1 μL) on a gradient surface inclined 15° from the horizontal plane[34] (reproduced with permission from the American Association for the Advancement of Science). (C) Video image showing fast movements of water drops (indicated by the plume- and streaklike appearances) resulting from the condensation of steam on a silicon wafer possessing a radial gradient (1 cm diameter) of surface energy[167] (reproduced with permission from the American Association for the Advancement of Science). (D, Top) Schematic showing the motion of a liquid droplet on flat (left) and porous (right) surfaces. (Bottom) Capillary number ($Ca = \upsilon\eta/\gamma$) as a function of the normalized drop radius ($R^* = R\ \partial\cos(\theta)/\partial x$) associated with the motion of a droplet of deionized water along the 1H,1H,2H,2H-perfluorodecyltrichlorosilane (tF8H2) molecular gradient created on top of flat (open symbols) and porous (solid symbols) silicon substrates. During the course of the experiment, the drop velocity was collected at multiple positions on the sample. The data presented have been compiled from the drop velocity data collected at the constant advancing contact angle of water equal to 70° (▽), 65° (△), 60° (◇), 100° (■), and 80° (●). The lines are meant to guide the eye[170] (reproduced with permission from the American Chemical Society).

about the kinetics of polymerization on surfaces in a very systematic and facile manner. Finally, gradients are conveniently suited to screen some important physicochemical phenomena. One example, out of many, involves studies of protein adsorption on surfaces where the grafted polymer brush density or length (or the combination of both, in case of orthogonal gradients) varies continuously and independently across the substrate. The main advantage of gradient structures in studying a complex phenomenon, such as protein adsorption, is that the monotonic variation of the physicochemical characteristics of the underlying gradient eliminates the requirement for interpolation to determine the surface response and enables an unambiguous interpretation of adsorption experiments. Below we discuss gradient functionality in terms of three important subattributes concerning the ability to (1) drive, (2) record, and (3) screen a phenomenon.

6.1. Driving a Phenomenon. The utilization of gradients in transporting liquids across surfaces has been demonstrated in multiple studies. The basic premise for moving a droplet is associated with creating a gradient in the interfacial tension at the front and back edges of the drop acting at the droplet/substrate/air interface (Figure 8A). Chaudhury and Whitesides studied the motion of water droplets on a surface of varying hydrophobicity formed by coating a silicon wafer partially with *n*-decyltrichlorosilane (Figure 8B).[34] A drop of water moved from the hydrophobic toward the hydrophilic end of the wafer; this occurred only very slowly and only over a small distance (on the order of a few millimeters). Much higher drop speeds have been observed recently for small water droplets formed by the condensation of steam onto a gradient surface (Figure 8C), [167] by vibrating the surface,[168,169] by rolling the drop on a rough substrate decorated with a chemical gradient made of hydrophobic organosilane modifiers on rough substrates (Figure 8D),[170] and on wettability gradients prepared by embossing topographical patterns in soft waxes.[171] Recent years witnessed a large body of work pertaining to the investigation of liquid motion due to "static gradients".[172,173] A comprehensive account of these

(167) Daniel, S.; Chaudhury, M. K.; Chen, J. C. *Science* **2001**, *291*, 633−636.
(168) Daniel, S.; Chaudhury, M. K. *Langmuir* **2002**, *18*, 3404−3407.
(169) Daniel, S.; Sircar, S.; Gliem, J.; Chaudhury, M. K. *Langmuir* **2004**, *20*, 4085−4092.
(170) Petrie, R. J.; Bailey, T.; Gorman, C. B.; Genzer, J. *Langmuir* **2004**, *20*, 9893−9896.
(171) Zhang, J.; Han, Y. *Langmuir* **2007**, *23*, 6163−6141.
(172) Subramanian, R. S.; Moumen, N.; McLaughlin, J. B. *Langmuir* **2005**, *21*, 11844−11849.

investigations is beyond the scope of this brief report, so we refer the interested reader to the existing literature.[174−178] Bain[179] and Ondarçuhu[180] showed independently that rapid motion (speed >5 cm/s) over long distances (many centimeters) could be achieved if a gradient in wettability was created dynamically by a chemical reaction at the drop/surface interface. More detailed accounts of the self-propelled motion of liquids can be found in recent publications.[181,182]

Much better control over drop motion can be achieved by varying the gradient in interfacial tension acting on the front and back of the droplet by applying an external field. The utilization of diverse approaches from electrochemistry, photochemistry, electrocapillarity, and thermochemistry have not only allowed us to overcome the aforementioned deficiencies of static gradients but has also enabled complete control over the directionality (forward vs reverse) of the gradients and thus the directionality of a gradient-driven phenomenon. For instance, Abbott and co-workers reported on the development of a redox-active surfactant based on ferrocene (Fc).[183] The oxidized form, $Fc^{+}(CH_2)_{11}N^{+}(CH_3)_3Br^{-}$, has charged groups at both ends of the hydrocarbon chain and is well solvated by water. The reduced form, $Fc(CH_2)_{11}N^{+}(CH_3)_3Br$, is surface-active and lowers the surface tension of the aqueous solution. The electrochemical reduction of ferrocinium to ferrocene here generates a surface tension gradient that can be used to pump liquids reversibly along a channel. Abbott et al. also demonstrated electrochemically induced dewetting with the same surfactant system and proposed that the driving force was a change in the adsorption of the surfactant at the solid−liquid interface.

Another example involves the well-studied light-induced cis/trans isomerization of azobenzene. Ichimura and co-workers created real-time wettability spatial patterns on flat surfaces by using azobenzene-based derivatives (specifically, calixresorcinarene modified with four azobenzene chains[184]). By irradiating surfaces covered with SAMs of the aforementioned moiety with UV light, the surfaces became wettable. By exposing the surface to blue light, the azobenzene flipped back to the trans conformation, thus making the substrate less wettable. By asymmetrically irradiating the substrate with UV and blue light, a wettability gradient was generated that was capable of moving liquids along the substrate. Unfortunately, the rather high contact angle hysteresis present in the system did not enable the motion of polar liquids. Only hydrophobic liquids, such as olive oil, were transported with velocities of ∼50 μm/s. Shin and Abbott demonstrated that the photoisomerization of azobenzene-containing surfactants could also be used to control the dynamic surface tension of aqueous interfaces, providing another route to light-induced Marangoni effects.[185] Berná and co-workers recently reported on creating synthetic molecular motors that converted light into biased Brownian molecular motion of stimuli-responsive rotaxanes to expose or conceal fluoroalkane residues, thereby modifying the surface tension.[186] The research team demonstrated that the collective operation of a monolayer of the "molecular shuttles" was sufficient to power the transportation of a microliter droplet of diiodomethane on inclined planes. Finally, Brochard, Cazabat, and co-workers demonstrated that a small stationary temperature gradient across the substrate was also able to drive a liquid across the substrate.[159−162]

Chemical reactions can drive not only the motion of liquids but also can govern the movement of larger molecules, such as dendrimers.[187] Chang and co-workers recently demonstrated this concept by using amine-terminated dendrimer molecules that were placed onto aldehyde-covered substrates (Figure 9A). The motility was driven by the ability of the amine group to attach to the aldehyde functionality by imine condensation reaction. The imine groups can readily hydrolyze, thus liberating the dendrimer from the bound position on the substrate. Whereas on a substrate decorated homogeneously with the aldehyde molecules the locomotion of dendrimers occurs in random directions, one can direct the movement of the adsorbates by depositing them onto substrates bearing a density gradient of the aldehyde groups. Chang and co-workers prepared such aldehyde gradients by gradually immersing glass slides into solutions containing organosilane-based aldehydes and demonstrated that amine-terminated dendrimers moved in the direction containing a larger concentration of aldehyde groups on the surface.

Surface-bound gradients have also been used as "engines" capable of driving biological moieties. Over the past few decades, multiple studies have been published that reported on the response of living cells (orientation and migration) to the variation of chemistry (chemotaxis, haptotaxis),[31,188,189] light intensity (phototaxis),[190] electrostatic potential (galvanotaxis),[191,192] gravitational field (geotaxis),[193] and mechanical properties (durotaxis) (Figure 10A,B).[104,106] Many of those studies employed either static or dynamic gradients in physicochemical properties or micropatterned arrays of asymmetric regions of sticky groups on the substrate[194] that governed the locomotion of cells (Figure 10C). Rather than providing a detailed account of these investigations, we refer the interested reader to the existing literature on this topic and recent work that partially reviews the progress in the field.[194] In our discussion here, we restrict ourselves only to the cases involving the locomotion of cells due to surface-bound polymer gradients and UV light.

Ionov and co-workers prepared gradients of kinesin by adsorbing kinesin onto PEG-based surface-bound gradients (Figure 9B).[123] Microtubules adsorbed onto such substrates glided over the kinesin gradients with a constant velocity. The presence of a kinesin concentration gradient also facilitated microtubule sorting: whereas smaller microtubules occupied only regions with a high kinesin concentration, larger microtubules could adsorb onto substrate sites covered with a smaller concentration of kinesin. In a follow-up study, Ionov and co-workers subsequently extended their previous work by fabricating gradients comprising responsive substrate-bound brushes made of PNIPAAm, which were backfilled with kinesin molecules.

(173) Moumen, N.; Subramanian, R. S.; McLaughlin, J. B. *Langmuir* **2006**, *22*, 2682−2690.
(174) Bain, C. D. *ChemPhysChem* **2001**, *2*, 580−582.
(175) Suda, H.; Yamada, S. *Langmuir* **2003**, *19*, 529−531.
(176) Shastry, A.; Case, M. J.; Böhringer, K. F. *Langmuir* **2006**, *22*, 6161−6167.
(177) Pismen, L. M.; Thiele, U. *Phys. Fluids* **2006**, *18*, 042104-1−042104-10.
(178) Kay, E. R.; Leigh, D. A.; Zerbetto, F. *Angew. Chem., Int. Ed.* **2007**, *46*, 72−191.
(179) Bain, C. D.; Burnett-Hall, G.; Montgomerie, R. *Nature* **1994**, *372*, 414−415.
(180) Dos Santos, F. D.; Ondarçuhu, T. *Phys. Rev. Lett.* **1995**, *75*, 2972−2975.
(181) John, K.; Bär, M.; Thiele, U. *Eur. Phys. J. E* **2005**, *18*, 183−199.
(182) Nagi, K.; Sumino, Y.; Yoshikawa, K. *Colloids Surf., B* **2007**, *56*, 197−200.
(183) Gallardo, B. S.; Gupta, V. K.; Eagerton, F. D.; Jong, L. I.; Craig, V. S.; Shah, R. R.; Abbott, N. L. *Science* **1999**, *283*, 57−60.
(184) Ichimura. K.; Oh, S. K.; Nakagawa. M. *Science* **2000**, *288*, 1624−1626.
(185) Shin, J. Y.; Abbott, N. L. *Langmuir* **1999**, *15*, 4404−4410.
(186) Berná, J.; Leigh, D. A.; Lubomska, M.; Mendoza, S. M.; Pérez, E. M.; Rudolf, P.; Teobaldi, G.; Zerbetto, F. *Nat. Mater.* **2005**, *4*, 704−710.
(187) Chang, T.; Rozkiewicz, D. I.; Ravoo, B. J.; Meijer, E. W.; Reinhouldt, D. N. *Nano Lett.* **2007**, *7*, 978−980.
(188) Carter, S. B. *Nature* **1967**, *213*, 256 −260.
(189) Pettit, E. J.; Fay. F. S. *Physiol. Rev.* **1998**, *78*, 949−967.
(190) Saranak, J., Foster. K. W. *Nature* **1997**, *387*, 465−466.
(191) Erickson, C. A.; Nuccitelli, R. *J. Cell Biol.* **1984**, *98*, 296−307.
(192) Brown, M. J.; Loew, L. M. *J. Cell Biol.* **1994**, *127*, 117−128.
(193) Lowe, B. *J. Exp. Biol.* **1997**, *200*, 1593−1606.
(194) Kumar, G.; Ho, C.-C.; Co, C. C. *Adv. Mater.* **2007**, *19*, 1094−1090.

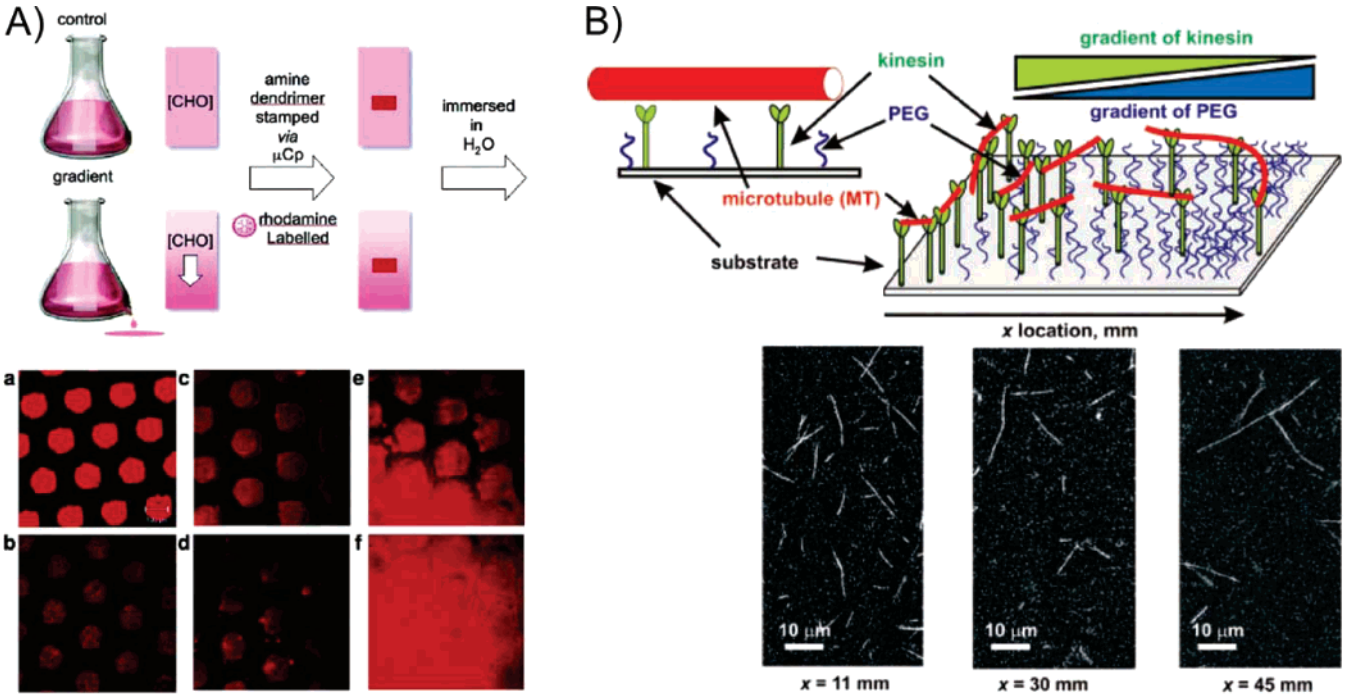

Figure 9. (A, Top) Method for transporting anime-terminated dendrimer molecules on top of aldehyde-covered substrates. (Bottom) Confocal microscope images of dendrimers stamped using microcontact printing with circles ~100 μm in diameter: (a) before immersion; (b) a uniform aldehyde substrate; and (c−f) gradient substrates with increasing aldehyde concentrations after 16 h of immersion in water[187] (reproduced with permission from the American Chemical Society). (B) Gliding motility of microtubules on a poly(ethylene glycol) (PEG)-gradient surface with immobilized kinesin. (Top) Schematic diagram of the motility system. Because the grafting density of PEG increases from left to right, the kinesin gradient is formed in the opposite direction. (Bottom) Fluorescence micrographs of gliding microtubules taken at three different locations along the gradient surface. At lower kinesin density, the number of microtubules per field of view decreases, whereas the average length of the microtubules increases[123] (reproduced with permission from the American Chemical Society).

The motility of microtubules was tailored by varying the temperature of aqueous solution from below (27 °C) to above (35 °C) the collapse temperature of PNIPAAm ($T_C \approx 32$ °C). The conformational changes of PNIPAAm brushes controlled the density of the exposed kinesin molecules and consequently the landing density and gliding velocity or repellency of microtubules. At low temperature, the PNIPAAm brush was in expanded state; it overshadowed the kinesin molecules, resulting in a lower adsorption of microtubules. However, at higher temperature PNIPAAm collapsed, thus exposing the kinesin molecules, which resulted in increased adsorption of microtubules.[195] Vogel and co-workers reported on creating molecular shuttles by creating kinesin arrays that served as tracks for sliding microtubules that, if equipped with biotin, can attach and carry any biomolecular cargo tagged with avidin groups.[196] The researchers developed methods for dynamically controlling the microtubule locomotion by utilizing caged adenosine triphosphate (ATP) molecules in conjunction with enzymatic ATP degradation by hexokinase. By exposing the system to UV light, ATP molecules were released, which powered the kinesin and turned on the "shuttle service" provided by the microtubules. The motion eventually ceased because hexokinase consumed all available ATP. Another brief exposure to UV light released more ATP, and the process continued. Modeling of the behavior of molecular motors has also been the focus of some published work.[197]

6.2. Recording a Phenomenon. Gradient geometries are conveniently suited as a medium for recording some physical phenomenon, such as adsorption, reaction, polymerization, and others. Our group has utilized this gradient attribute in several instances, and these are described in more detail below. For example, Tomlinson and co-workers used the gradient geometry to study the kinetics of the surface-initiated polymerization of poly(methyl methacrylate) (Figure 11A).[96,130] The rate of polymerization was found to obey the predicted dependence on the concentration of the activator and deactivator species in the polymerization mixture. Moreover, the gradient arrangement facilitated a methodical investigation of the "living" nature of the macroinitiator in the surface-initiated ATRP.[96] Shovsky and Schönherr utilized gradient geometry to monitor the kinetics and temperature dependence of the surface reactions of the alkaline hydrolysis of 11,11′-dithiobis(*N*-hydroxysuccinimidylundecanoate) SAMs on gold as well as the ester hydrolysis in SAMs of disulfides such as 11,11′-dithiobis(*tert*-butylundecanoate) (Figure 11B).[198] The reaction kinetics, rate constants, activation energies, and entropies were determined. Morgenthaler studied the formation of density gradients of poly(L-lysine)-*graft*-poly(ethylene glycol) copolymers onto metal oxide substrates by gradually immersing the substrate in the copolymer solution.[199] Our group has recently performed meticulous studies of polymer adsorption by gradually pouring polymer solution into a chamber containing a vertically standing silicon wafer.[200] The amount of adsorbed polymer, poly(styrene-*co*-4-bromostyrene, (PBr_xS, where x is the mole fraction of 4-bromostyrene), varied as a function of the position on the silica substrate. This allowed the authors to deduce the kinetics of adsorption of PBr_xS. A similar

(195) Ionov, L.; Stamm, M.; Diez, S. *Nano Lett.* **2006**, *6*, 1982−1987.
(196) Hess, H.; Clemmens, J.; Qin, D.; Howard, J.; Vogel, V. *Nano Lett.* **2001**, *1*, 235−239.
(197) Nitta, T.; Tanajashi, A.; Hirano, M.; Hess, H. *Lab Chip* **2006**, *6*, 881−885.
(198) Shovsky, A.; Schönherr, H. *Langmuir* **2005**, *21*, 4393−4399.
(199) Morgenthaler, S.; Zink, C.; Städler, B.; Vörös, J.; Lee, S.; Spencer, N. D.; Tosatti, S. G. P. *Biointerphases* **2006**, *1*, 156−165.
(200) Jhon, Y. K., Genzer, J. To be submitted for publication.

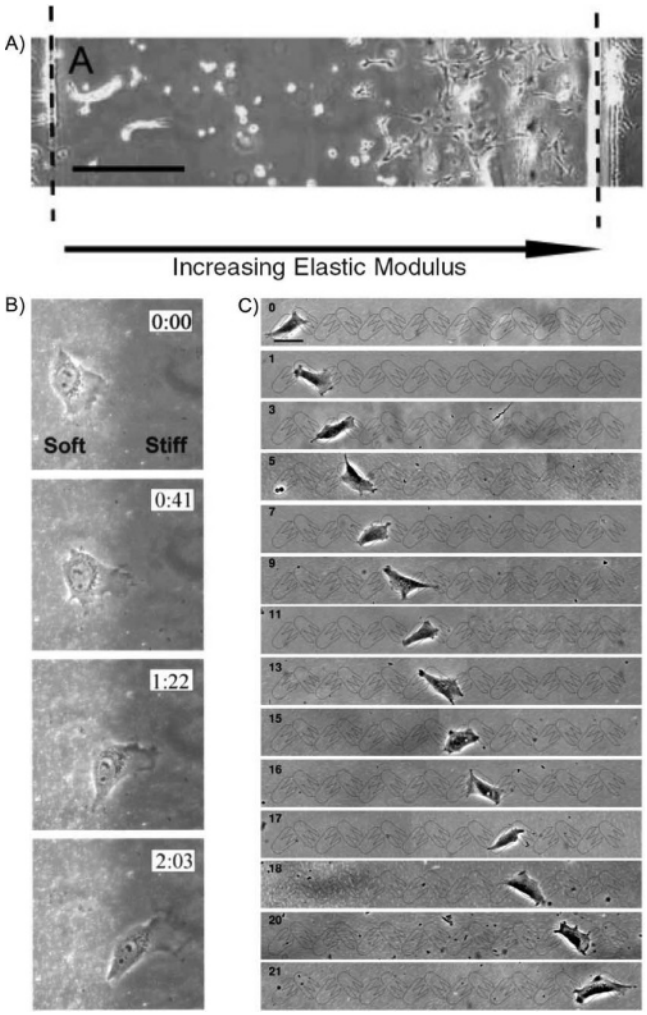

Figure 10. (A) Vascular smooth muscle cells spreading on poly(acrylamide) toward the region of higher stiffness/modulus.[106] (reproduced with permission from Wiley). (B) Movement of National Institutes of Health 3T3 (NIH T3T) cells on substrates with a rigidity gradient. Images were recorded with simultaneous phase and fluorescence illumination. Changes in substrate rigidity can be visualized as changes in the density of embedded fluorescent beads. A cell moved from the soft side of the substrate toward the rigid side by turning 90°. Note the increase in spreading area as the cell passed the boundary. Scale bar: 40 μm[104] (reproduced with permission from the Biophysical Society). (C) Time-lapse phase-contrast images (in hours) showing the continuous directional migration of a single NIH 3T3 fibroblast over a zigzag pattern on the substrate. The cell conforms to the individual islands as it moves continuously from left to right. Scale bar: 50 μm[194] (reproduced with permission from Wiley).

setup was utilized to understand the formation of surface-bound random copolymers of PBr_xS by gradually brominating surface-bound polystyrene chains. By varying the kind of solvent and the reaction temperature, the resulting PBr_xS chains had random or random-blocky character.[201] Van de Steeg and Gölander studied the adsorption of pluronics (PEO-PPO-PEO triblock copolymers) onto wettability gradients[202] prepared by the method discussed in ref 33. Higher adsorption of the copolymer was detected on the hydrophobic sides of the gradients, suggesting that the PPO block was responsible for the adsorption. Combinatorial substrates comprising surface-grafted polymer brushes have been used to monitor the swelling/collapse of copolymer blocks with selective solvents.[95,135,203] Several studies have demonstrated the suitability of combinatorial approaches to study the coalescence of droplets on chemically heterogeneous gradient substrates,[204] order−disorder transition in grafted oligoalkanes on surfaces,[38] and phase separation in immiscible homopolymer blends.[205] We have recently made use of gradient geometry to comprehend the mechanism of formation of SAMs made of organosilane precursors. Specifically, we provided evidence that depending on the nature of the end group in the semifluorinated organosilanes (SFO) and the vapor phase (humid air vs nitrogen atmosphere) the SFO molecules added themselves to the existing SAMs either as individual molecules or as multimolecular complexes (Figure 5B).[5,6,35] By making careful observations of the growth of gradient SAMs, Douglas, Genzer, and co-workers have found that the mechanism involved in forming molecular gradients by the vapor diffusion technique depends on the geometry of the diffusing system (Figure 5A).[206] Specifically, they discovered that in confined systems the molecules did not order themselves in a classical diffusionlike manner but grew in a wavelike fashion that spread out from a source point. The results should be important to the understanding of various self-propagating chemical reactions and self-assembly phenomena occurring in confined environments such as thin films and porous internal geometries of many materials (e.g., rocks, cement).

6.3. Screening a Phenomenon. Examining the structure of organic films has always been of paramount interest for producing soft materials with well-defined structure and properties. Gradient methodologies have played a key role in screening various characteristics of soft structures made of oligomeric and polymeric components. For instance, gradient geometries have been used to probe the development of topologies in thin block copolymer films (Figure 12A).[87,207,208,209] These studies enabled the systematic investigation of island/hole/flat surface transitions over a wide range of film thicknesses. Combinatorial methods based on gradient geometries have also been used to understand the phase behavior in polymer blends (Figure 12B,C)[85] or crystallization in thin polymer films. For instance, Beers and co-workers utilized gradient geometries in studying the crystallization growth rate and morphology in thin films of isotactic polystyrene,[210] and Walker and co-workers reported an investigation of the crystallization behavior in thin polypropylene films.[211] Several studies also reported on using substrates with gradients in wettability for studying the stability of liquids[212] and thin polymer films (i.e., dewetting) (Figure 12D).[48,85,86,208,213,214] Many research

(201) Semler, J. J.; Jhon, Y. K.; Tonelli, A.; Beevers, M.; Krishnamoorti, R.; Genzer, J. *Adv. Mater.* **2007**, *19*, 2877−2883.
(202) Van de Steeg, L. M. A.; Gölander, C.-G. *Colloids Surf.* **1991**, *55*, 105−119.
(203) Xu, C.; Wu, T.; Drain, C. M.; Batteas, J. D.; Fasolka, M. J.; Beers, K. L. *Macromolecules* **2006**, *39*, 3359−3364.
(204) Zhao, H.; Beysens, D. *Langmuir* **1995**, *11*, 627−634.
(205) Genzer, J.; Kramer, E. J. *Europhys. Lett.* **1998**, *44*, 180−185.
(206) Douglas, J. F.; Efimenko, K.; Fischer, D. A.; Phelan, F. R.; Genzer, J. *Proc. Natl. Acad. Sci. U.S.A.* **2007**, *104*, 10324−10329.
(207) Smith, A. P.; Douglas, J.; Meredith, J. C.; Karim, A.; Amis, E. J. *J. Polym. Sci, Polym. Phys.* **2001**, *87*, 2141−2158.
(208) Smith, A. P.; Sehgal, A.; Douglas, J. F.; Karim, A.; Amis, E. J. *Macromol. Rapid. Commun.* **2003**, *24*, 131−135.
(209) Epps, T. H., III; DeLongchamp, D. M.; Fasolka, M. J.; Fischer, D. A.; Jablonski, E. L. *Langmuir* **2007**, *23*, 3355−3362.
(210) Beers, K. L; Douglas, J. F.; Amis, E. J.; Karim, A. *Langmuir* **2003**, *19*, 3935−3940.
(211) Walker, M. L.; Smith, A. P.; Karim, A. *Langmuir* **2003**, *19*, 6582−6585.
(212) Smith, J. T.; Viglianti, B. L.; Reichert, W. M. *Langmuir* **2002**, *18*, 6289−6293.
(213) Choi, S.-H.; Zhang Newby, B.-m. *Langmuir* **2003**, *19*, 1419−1428.
(214) Ashley, K. M.; Ragavan, D.; Douglas, J. F.; Karim, A. *Langmuir* **2005**, *21*, 9518−9523.
(215) Morganthaler, S. M.; Lee, S.; Spencer, N. D. *Langmuir* **2006**, *22*, 2706−2711.

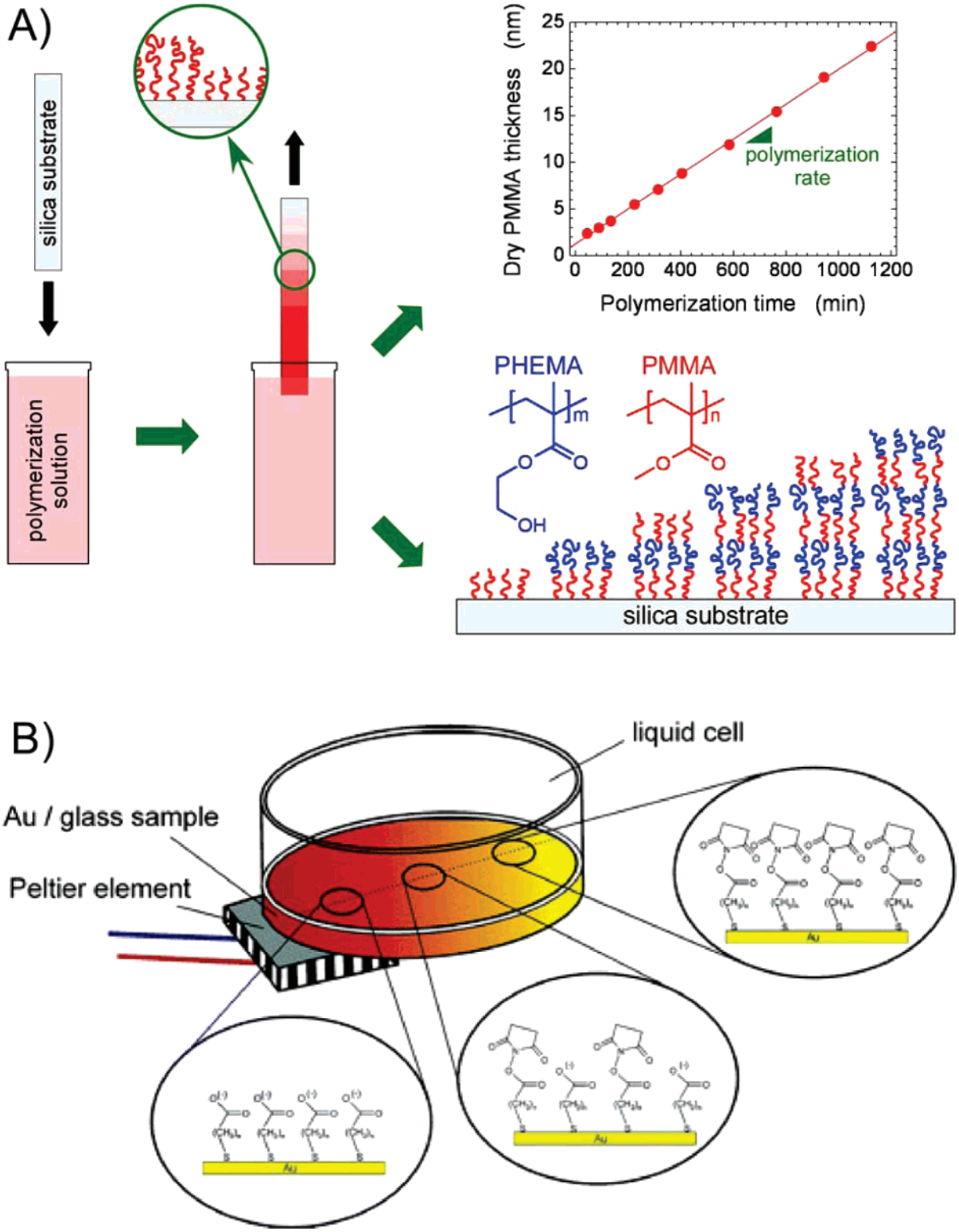

Figure 11. (A) Formation of polymer brushes on solid substrate via the grafting-from method following the dipping methodology results in polymer brush assemblies with molecular weight gradients. This method facilitates the study of polymerization kinetics and the formation of multiblock copolymer brush coatings[96] (reproduced with permission from the American Chemical Society). (B) Experimental setup used to monitor the kinetics and temperature dependence of surface reactions of alkaline hydrolysis of 11,11′-dithiobis(*N*-hydroxysuccinimidylundecanoate) SAMs on gold as well as ester hydrolysis in SAMs of disulfide 11,11′-dithiobis(*tert*-butylundecanoate)[198] (reproduced with permission from the American Chemical Society).

groups utilized molecular gradients comprising surface-grafted oligomers to study the order−disorder transition in short alkane-[38,215,216] and oligo(ethylene glycol)-based molecules on surfaces (Figure 13A).[38,217] In addition, substrates decorated with wettability gradients have been employed to probe the orientation of several liquid-crystalline materials (Figure 13B).[218,219] Finally,

(216) Venkataraman, N. V.; Zürcher, S.; Spencer, N. D. *Langmuir* **2006**, *22*, 4184−4189.

(217) Riepl, M.; Östblom, M.; Lundström, I.; Svensson, S. C. T.; van der Gon, A. W. D.; Schäferling, M.; Liedberg, B. *Langmuir* **2005**, *21*, 1042−1050.

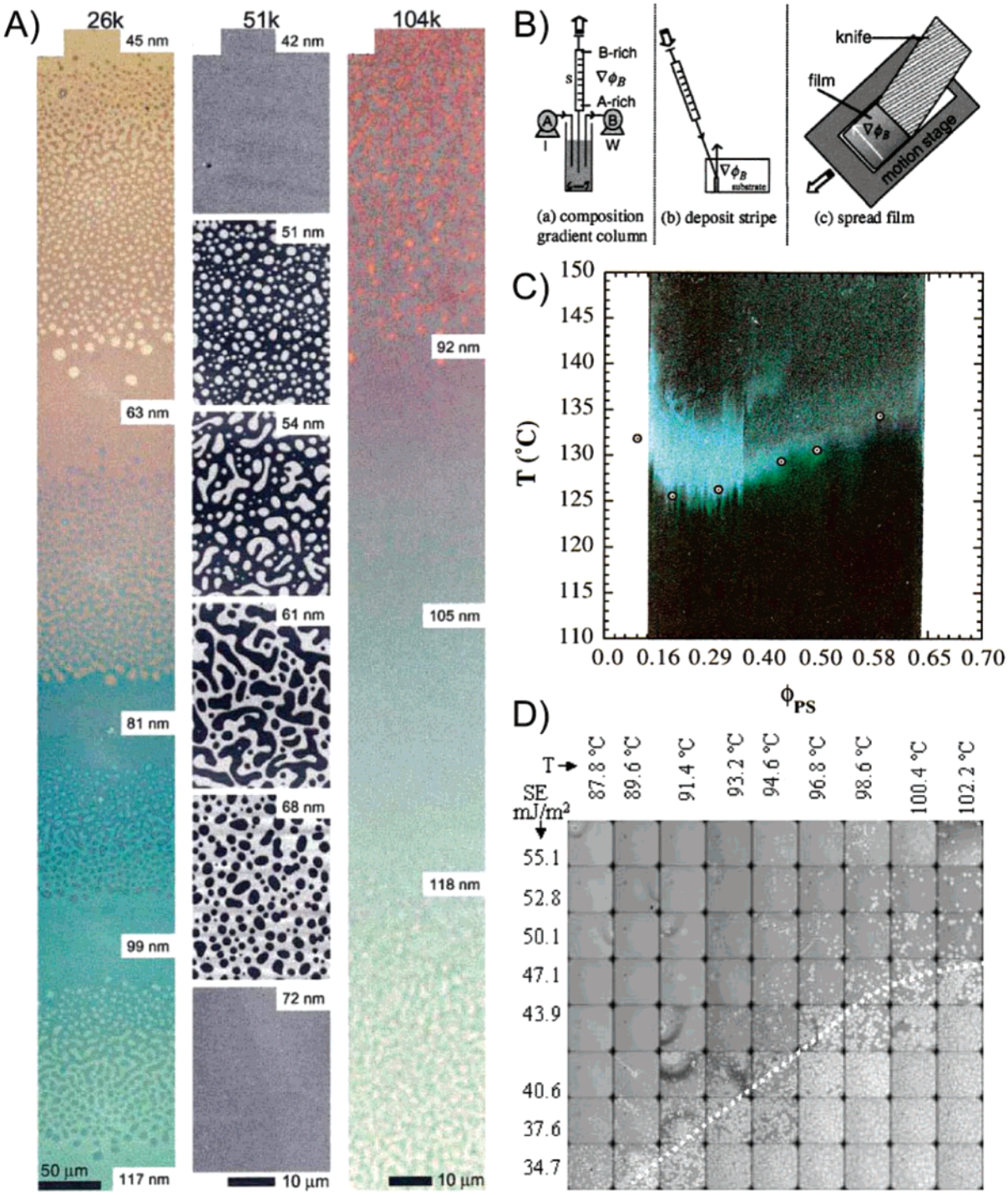

Figure 12. (A, Left) True color optical micrographs of a 26K poly(styrene-*block*-methyl methacrylate) block copolymer (PS-*b*-PMMA) film having a gradient in thickness from 45 to 117 nm. The sample was annealed for 6 h at 170 °C, and four successive lamellae are shown. (Middle) AFM micrographs (white corresponds to thicker topography) of a 51K PS-*b*-PMMA gradient film annealed 6 h at 170 °C. Images show the evolution of the surface morphology. (Right) True color optical micrograph of a 104K PS-*b*-PMMA gradient film annealed for 22 h at 170 °C showing a smooth region between the cessation of holes (orange, top) and the initiation of islands (green/yellow, bottom). The smooth region changes in color from purple to blue/green, indicating a change in thickness of approximately 25 nm[87] (reproduced with permission from the American Physical Society). (B) Schematic of the knife-edge coating method in conjunction with the composition gradient film coating procedure (reproduced with permission from the American Chemical Society).[85] (C) Lower critical solution temperature (LCST) cloud-point curve on a 2D PS/PVME blend film library on a Si−H substrate after 2 h of annealing on the temperature gradient stage. The library cloud-point curve agrees well with cloud points (circles with dots) measured independently with laser light scattering. The overall sample dimensions are 30 mm × 40 mm[85] (reproduced with permission from the American Chemical Society). (D) Combinatorial map of wetting and dewetting regions of a polystyrene film (M = 1800 g/mol) with an initial thickness of 37.5 nm and a range of temperatures and surface energies. The PS film was dewetted for 50 min; the magnification of the image was 20×. The dashed line is the dewetting−wetting line[214] (reproduced with permission from the American Chemical Society).

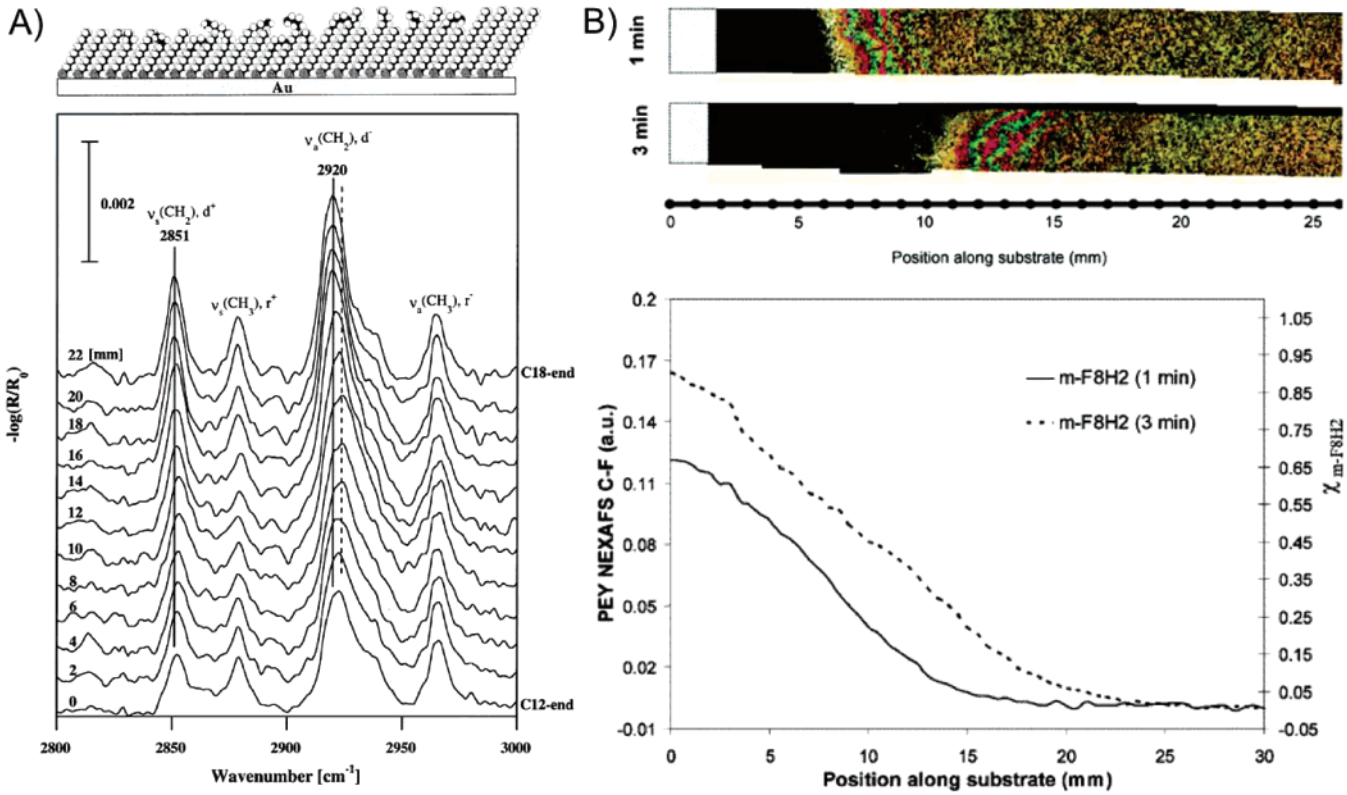

Figure 13. (A) Schematic depiction of a order/disorder gradient $HS(CH_2)_{11}CH_3/HS(CH_2)_{17}CH_3$ (C12/C18) on gold. Infrared reflection absorption spectroscopy (IRAS) spectra for C12/C18 gradients in the high-frequency region. The step length along the gradient between each spectrum is 2 mm[38] (reproduced with permission from Elsevier). (B, Bottom) Partial electron yield (PEY) near-edge X-ray absorption fine structure (NEXAFS) spectroscopy signal (C−F 1s → σ^* transition) recorded as a function of position along each sample for surface gradients prepared from 1H,1H,2H,2H-perfluorodecyldimethylchlorosilane (mF8H2). (top) Optical appearances of liquid crystals (when viewed using reflectance-mode polarized light microscopy) in contact with surface gradients prepared from mF8H2[218] (reproduced with permission from the American Chemical Society).

gradient methodologies have also been utilized to optimize the structure of organic light-emitting diodes by gradually varying the material thickness[58,59] or orthogonally varying the thickness and chemistry.[220]

Gradient geometries are conveniently suited to the investigation of adsorption of inorganic or organic nano-objects. One of the areas that has received a considerable attention from our group and other involves the adsorption and assembly of nanoparticles. To this end, we used organosilane evaporation methods to create a chemical gradient, which was subsequently used as a template to produce number density gradients of nanoparticles that attached electrostatically to the underlying chemical gradient motif made of oligomers (Figure 14A) or polymers (Figure 14B,C).[145−147,221] Song and co-workers formed nanoparticle density patterns by first forming hydrophobic radial gradients using the method developed earlier by Choi et al.,[48] backfilling the empty sites on the surface with amine-terminated organosilane to which they attached fluorescently labeled PS beads (diameter ≈100 nm).[222] Wang and co-workers also prepared nanoparticle-filled polymer gradients by electropolymerization of acrylamide and filling the polymeric skeleton with gold nanoparticles (Figure 14D).[137] Bhat and Genzer established that the particle distribution inside polymer brushes is governed by the interplay between the particle size and the grafting density and the molecular weight of the surface-tethered polymer,[145] thus verifying earlier theoretical predictions of Kim and O'Shaughnessy.[223] Studies on the systematic adsorption of nonspherical particles have also been reported. For instance, Myung and co-workers used molecular density gradients to assemble V_2O_5 nanowires.[224]

Probing the mechanical properties of materials is one of the chief tenets of materials research. Gradient geometries have played a chief role in the measurement of mechanical characteristics of soft materials. Taking a cue from nature (specifically, the structure of a byssus, a tissue through which mussels attach to hard objects such as stones), Waite and co-workers discussed the application of designed structures enabling a gradual transition from hard to soft tissues by self-assembling diblock copolymers displaying a "non-collagenic" block and a "stiffness tunable" block made up of either elastin-like (soft) or amorphous polyglycine (intermediate) or a silklike (hard) material.[225] The individual copolymers in such modulus-graded threads were held together via metal binding through histidine-rich sequences present at both the $-NH_2$ and −COOH termini of the diblock copolymers. Stafford and co-workers introduced a new measurement technique coined strain-induced elastic buckling instability for mechanical measurements (SIEBIMM), which utilized wrinkling in thin films to determine the modulus of the skin material. They deposited

(218) Clare, B. H.; Efimenko, K.; Fischer, D. A.; Genzer, J.; Abbott, N. L. *Chem. Mater.* **2006**, 18, 2357−2363.
(219) Price, A. D.; Schwartz, D. K. *Langmuir* **2006**, *22*, 9753−9759.
(220) Gross, M.; Müller, D. C; Nothofer, H.-G.; Scherf, U.; Neher, D.; Braüchle, C.; Meerholz, K. *Nature* **2000**, *405*, 661−665.
(221) Bhat, R. R.; Fischer, D. A.; Genzer, J. *Langmuir* **2002**, *18*, 5640−6543.
(222) Song, F.; Cai, Y.; Zhang Newby B.-m. *Appl. Surf. Sci.* **2006**, *253*, 2393−2398.
(223) Kim, J. U.; O'Shaughnessy, B. *Phys. Rev. Lett.* **2002**, *89*, 238301−238301-4.
(224) Myung, S.; Im, J.; Huang, L.; Rao, S. G.; Kim, T.; Lee, D. J.; Hong, S. *J. Phys. Chem. B* **2006**, *110*, 10217−10219.
(225) Waite, J. H.; Lichtenegger, H. C.; Stucky, G. D.; Hansma, P. *Biochemistry* **2004**, *43*, 7653−7662.

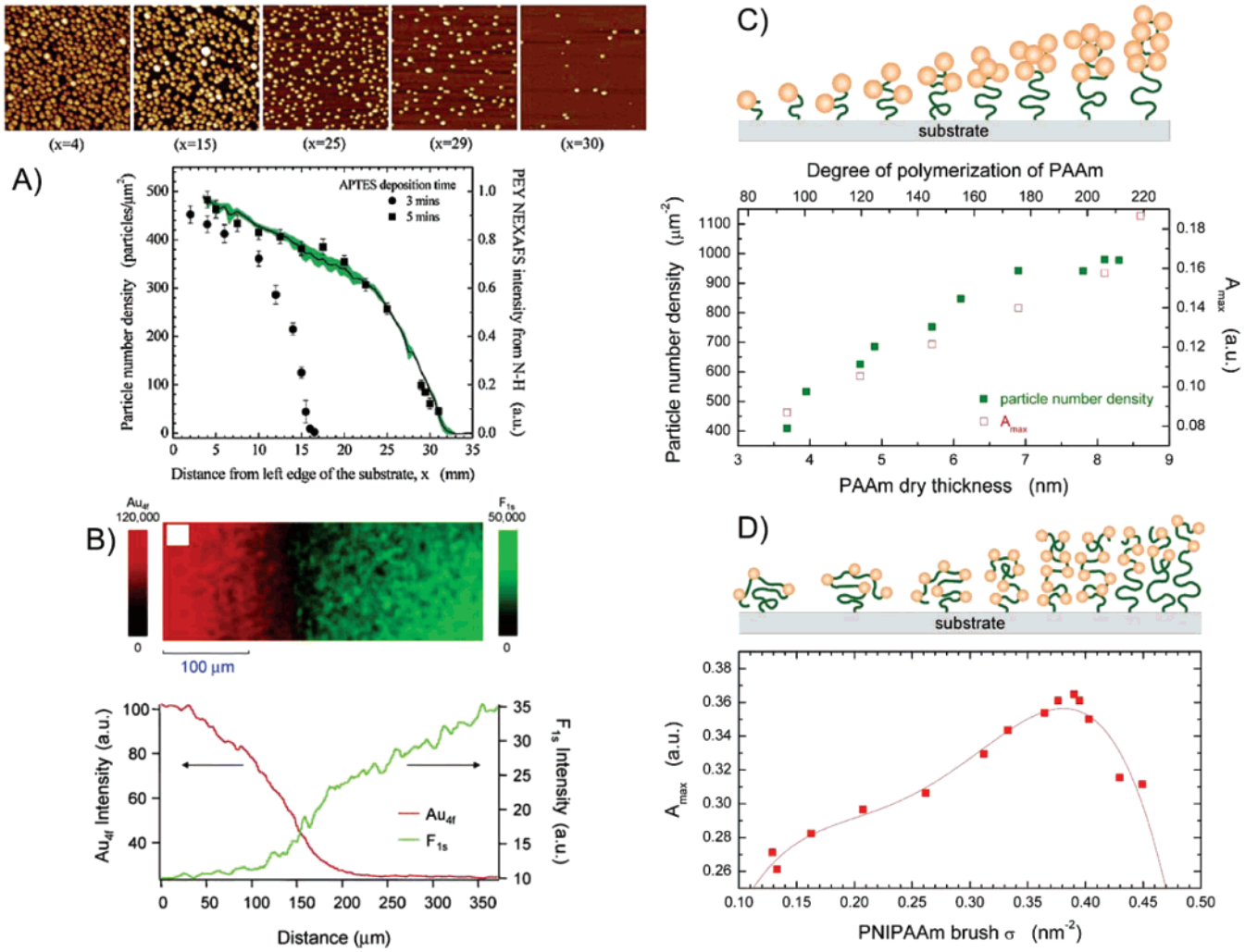

Figure 14. (A, Top) AFM images of gold particles adsorbed along a substrate prepared by evaporating an *n*-aminopropyl triethoxysilane (APTES)/paraffin oil (PO) mixture for 5 min followed by immersion in a 16-nm-diameter colloidal gold solution for 24 h (edge of each image = 1 μm). (Bottom) Particle number density profile (left) for two gradients prepared by evaporating APTES/PO mixtures for 3 (circles) and 5 (squares) min. The data points represent an average of three transverse scans along the gradient taken at the center of the sample (y = 0 mm) and at $y = -3$ and +3 mm. The line represents the partial electron yield (PEY) near-edge X-ray absorption fine structure (NEXAFS) spectroscopy profile (right) of N−H bonds from an ATEPS gradient prepared by evaporating an APTES/PO mixture for 5 min. The area around the PEY NEXAFS line denotes the measurement uncertainty (based on seven line scans along the gradient taken between −3 and +3 mm from the center of the sample)[221] (reproduced with permission from the American Chemical Society). (B) Particle number density (closed squares, left ordinate) and the maximum intensity of the gold plasmon peak (open squares, right ordinate) as a function of the dry thickness of the poly(acryl amide) (PAAm) brush (bottom abscissa) or alternatively the degree of polymerization of PAAm (top abscissa). The cartoon illustrates schematically the proposed distribution of the gold nanoparticles inside the PAAm brush[145] (reproduced with permission from Elsevier). (C) Intensity (A_{max}) of the gold plasmon peak in the UV−vis spectrum of 3.5 nm gold nanoparticles in poly(*N*-isopropyl acrylamide) (PNIPAAm) brushes as a function of the PNIPAAm grafting density (σ). The line is meant to guide the eye. The cartoon illustrates schematically the proposed distribution of the gold nanoparticles inside the PNIPAAm brush[145] (reproduced with permission from Elsevier). (D, Top) X-ray photoelectron spectroscopy image showing the transition region of a perfluorooctanoic acid (PFOA)-derivatized PAA thickness gradient. The gradient is visualized by depositing gold nanoparticles over this gradient and then measuring Au 4f and F 1s photoelectron intensities. Color scales for Au (left) and F (right) are given to the side of the image. Intermediate colors represent areas of the sample with mixed Au and F signals. (Bottom) Line scans showing the spatial distribution of the Au 4f and F 1s photoelectron intensities over the transition region[137] (reproduced with permission from the American Chemical Society).

a thickness gradient of PS on top of the PDMS substrate, and upon applying tensile strain to the sample, buckles developed that were oriented parallel to the direction of strain; the buckle periodicity increased with increasing thickness of the PS film.[7] This method provided an elegant way of determining the elastic modulus of other polymeric and nonpolymeric materials in a simple, reproducible manner.

Perhaps no other field has benefited from utilizing gradient geometries for screening properties more than bioscience. The reason is obvious because there are many parameters that affect the partitioning of biomolecules at surfaces and interfaces. To this end, molecular gradients have been utilized early on for systematic studies of the adsorption of surfactants (e.g., CTAB, SDS, $C_{12}E_5$, Tween 20),[10,32,226] bacteria (*Escherichia coli*, *Streptocuccus oralis*, *Streptococcus sobrinus*),[227,228] and proteins (e.g., γ-globulin, fibrinogen, lysozyme, IgG, high-molecular-weight kinogen, HSA, fibronectin, kinesin, laminin, collagen,

(226) Welin-Klinström, S.; Askendal, A.; Elwing, H. *J. Colloid Interface Sci.* **1993**, *158*, 188−194.
(227) Otto, K.; Elwing, H.; Hermansson, M. *Colloids Surf., B* **1999**, *15*, 99−111.
(228) Bos, R.; de Jonge, J. H.; van de Belt-Gritter, B.; de Vries, J.; Bisscher, H. J. *Langmuir* **2000**, *16*, 2845−2850.
(229) Elwing, H.; Askendal, A.; Lundström, I. *Prog. Colloid Polym. Sci.* **1987**, *74*, 103−107.

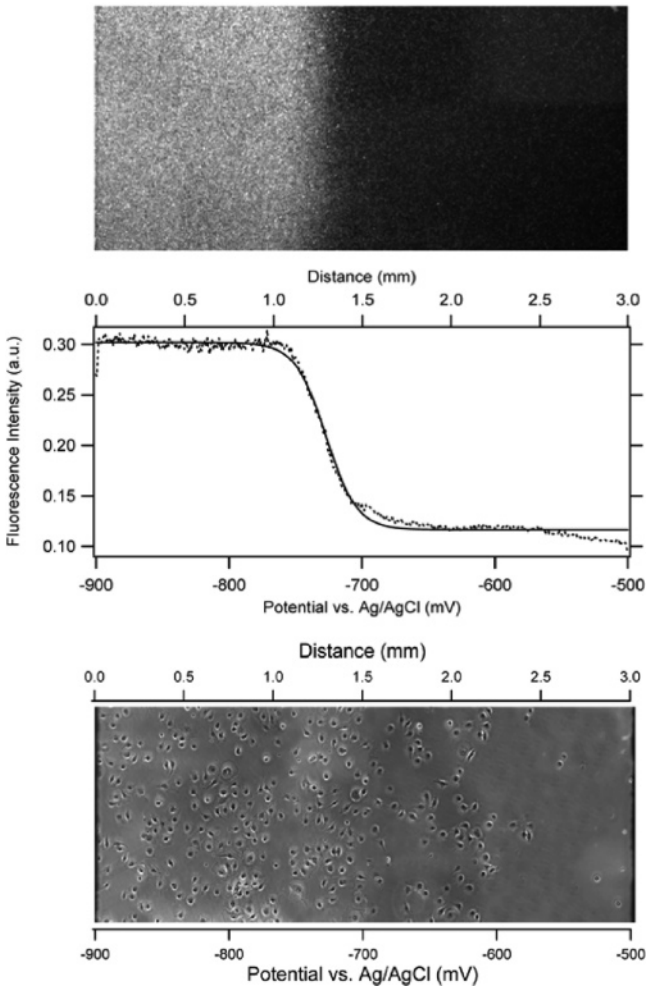

Figure 15. Fluorescence microscope image (top) and spatial intensity profile (middle) for the immobilization of amine-terminated fluorescent nanospheres onto an 11-mercaptoundecanoic acid (MUA)/11-mercaptoundecanol (MUD) gradient. The intensity profile is shown as a function of both the position across the film and the corresponding surface potential. (Bottom) Optical micrograph showing the adhesion of 3T3 fibroblast cells on a MUA/MUD-derived fibronectin (FN)/bone serum albumin (BSA) gradient[44] (reproduced with permission from the American Chemical Society).

biotin).[10,24,123,156,149,217,226,229−240] In addition, surface-bound gradients have also been used to investigate systematically platelet adhesion,[241,242] enzyme immobilization,[243] cell adhesion (Figures 15 and 16),[11,21,31,64,65,72−74,108,117,118,139,140,142,150,235,244−262] hybridization on biochips prepared by immobilized oligonucleotide density arrays,[69] and other phenomena involving interfacial biomaterial behavior on manmade surfaces. We realize that this account of employing gradients in biomaterial interfacial studies is far from complete. It would take another complete review to describe these studies properly.

Conclusions

The chief purpose of this feature article is to summarize advances made by us and many other groups around the world in generating and utilizing gradients of soft materials. Since their first creation, about half a century ago,[31] gradient surfaces have enjoyed tremendous growth. This is best documented by the almost exponential rise in the number of publications on the topic. Gradient surfaces have not only enabled the generation of "charming" surface motifs but more importantly, as documented in the article, have facilitated systematic studies of some physicochemical phenomena, have enabled the generation of smart/responsive materials, and have provided means of dynamically adjusting physicochemical aspects of surfaces. The field of material science involving the preparation and utilization of gradient surfaces has now evolved from an infant into a mature scientific discipline, thanks primarily to the numerous researchers from various scientific disciplines, many of whom are regular readers of and contributors to this journal. It is indeed interesting to note that a full 30% of the articles cited in this article have appeared in *Langmuir*! Our hope is that this article will not only provide a useful summary of up-to-date progress achieved by us and others but perhaps, more importantly, will stimulate more research and development in this rapidly growing field of materials science.

Acknowledgment. We are indebted to the former and current members of the Genzer research group and to our many colleagues all over the world with whom we have had the pleasure of

(230) Elwing, H.; Welin, S.; Askendal, A.; Lundström, I. *J. Colloid Interface Sci.* **1988**, *123*, 306−308.
(231) Elwing, H.; Askendal, A.; Lundström, I. *J. Colloid Interface Sci.* **1989**, *128*, 296−300.
(232) Gölander, C.-G.; Lin, Y.-S.; Hlady, V.; Andrade, J. D. *Colloids Surf.* **1990**, *49*, 289−302.
(233) Hlady, V. *Appl. Spectrosc.* **1991**, *45*, 246−252.
(234) Welin,-Klintström, S.; Lestelius, M.; Liedberg, B.; Tegvall, P. *Colloids Surf., B* **1999**, *15*, 81−87.
(235) Iwasaki, Y.; Sawada, S. i.; Nakabayashi, N.; Khang, G.; Lee, H. B.; Ishihara, K. *Biomaterials* **1999**, *20*, 2185−2191.
(236) Choee, J.-H.; Lee, S. J.; Lee, Y. M.; Rhee, J. M.; Lee, H. B. *J. Appl. Polym. Sci.* **2004**, *92*, 599−606.
(237) Smith, J. T.; Tomfohr, J. K.; Wells, M. C.; Beebe, T. P.; Kepler, T. B.; Reichert, W. M. *Langmuir* **2004**, *20*, 8279−8286.
(238) Kim, M. S.; Seo, K. S.; Khang, G.; Lee, H. B. *Langmuir* **2005**, *21*, 4066−4070.
(239) Kim, M. S.; Seo, K. S.; Khang, G.; Lee, H. B. *Bioconjugate Chem.* **2005**, *16*, 145−149.
(240) Elliot, J. T.; Woodward, J. T.; Umarji, A.; Mei, Y.; Tona, A. *Biomaterials* **2007**, *28*, 576−585.
(241) Lee, J. H.; Jeong, B. J.; Lee, H. B. *J. Biomed. Mater. Res.* **1997**, *34*, 105−114.
(242) Lee, J. H.; Lee, H. B. *J. Biomed. Mater. Res.* **1998**, *41*, 304−311.
(243) Loos, K.; Kennedy, S. B.; Eidelman, N.; Tai, Y.; Zharnikov, M.; Amis, E. J.; Ulman, A.; Gross, R. A. *Langmuir* **2005**, *21*, 5237−5241.
(244) Harris, A. *Exp. Cell Res.* **1973**, *77*, 285−297.
(245) McKenna, M. P.; Raper, J. A. *Dev. Biol.* **1988**, *130*, 232−236.
(246) Brandley, B. K.; Schnaar, R. L. *Dev. Biol.* **1989**, *135*, 74−86.
(247) Brandley, B. K.; Shaper, J. H.; Schnaar, R. L. *Dev. Biol.* **1990**, *140*, 161−171.
(248) Khang, G.; Lee, S. J.; Lee, J. H.; Kim, Y. S.; Lee, H. B. *Bio-Med. Mater. Eng.* **1999**, *9*, 179−187.
(249) Wigglesworth-Cooksey, B.; van der Mei, H.; Busscher, H. J.; Cooksey, K. E. *Colloids Surf., B* **1999**, *15*, 71−79.
(250) Lee, J. H.; Khang, G.; Lee, J. W.; Lee, H. B. *J. Colloid Interface Sci.* **1998**, *205*, 323−330.
(251) Khang, G.; Rhee, J. M.; Lee, J. H.; Lee, I. Lee, H. B. *Korea Polym. J.* **2000**, *8*, 276−284.
(252) Khang, G.; Choee, J.-H.; Rhee, J. M.; Lee, H. B. *J. Appl. Polym. Sci.* **2002**, *85*, 1253−1262.
(253) Lee, S. J.; Khang, G.; Lee, Y. M.; Lee, H. B. *J. Colloid Interface Sci.* **2003**, *259*, 228−235.
(254) Mei, Y.; Wu, T.; Xu, C.; Langenbach, K. J.; Elliot, J. T.; Vogt, B. D.; Beers, K. L.; Amis, E. J.; Washburn, N. R. *Langmuir* **2005**, *21*, 12309−12314.
(255) Simon, C. G., Jr.; Eidelman, N.; Kennedy, S. B.; Sehgal, A.; Khatri, C. A.; Washburn, N. R. *Biomaterials* **2005**, *26*, 6906−6915.
(256) Mitchell, S. A.; Poulsson, A. H. C.; Davidson, M. R.; Bradley, R. H. *Colloids Surf., B* **2005**, *46*, 108−116.
(257) Kennedy, S. B.; Washburn, N. R.; Simon, C. G., Jr.; Amis, E. J. *Biomaterials* **2006**, *27*, 3817−3824.
(258) Mei, Y.; Elliot, J. T.; Smith, J. R.; Langenbach, K. J.; Wu, T.; Xu, C.; Beers, K. L.; Amis, E. J.; Henderson, L. *J. Biomed. Mater. Res. A* **2006**, *79*, 975−988.
(259) Zapata, P.; Su, J.; Garcia, A. J.; Meredith, J. C. *Biomacromolecules* **2007**, *8*, 1907−1917.
(260) Kim, S. H.; Ha, H. J.; Ko, Y. K.; Yoon, S. J.; Rhee, J. M.; Kim, M. S.; Lee, H. B.; Khang, G. *J. Biomater. Sci., Polym. Ed.* **2007**, *18*, 609−622.
(261) Kim, M. S.; Shin, Y. N.; Cho, M. H.; Kim, S. H.; Kim, S. K.; Chi, Y. H.; Khang, G.; Lee, I. W.; Lee, H. B. *Tissue Eng.* **2007**, *13*, 2095−2103.
(262) Petty, R. T.; Li, H. W-.; Maduram, J. H.; Ismagilov, R.; Mrksich, M. *J. Am. Chem. Soc.* **2007**, *129*, 8966−8967.

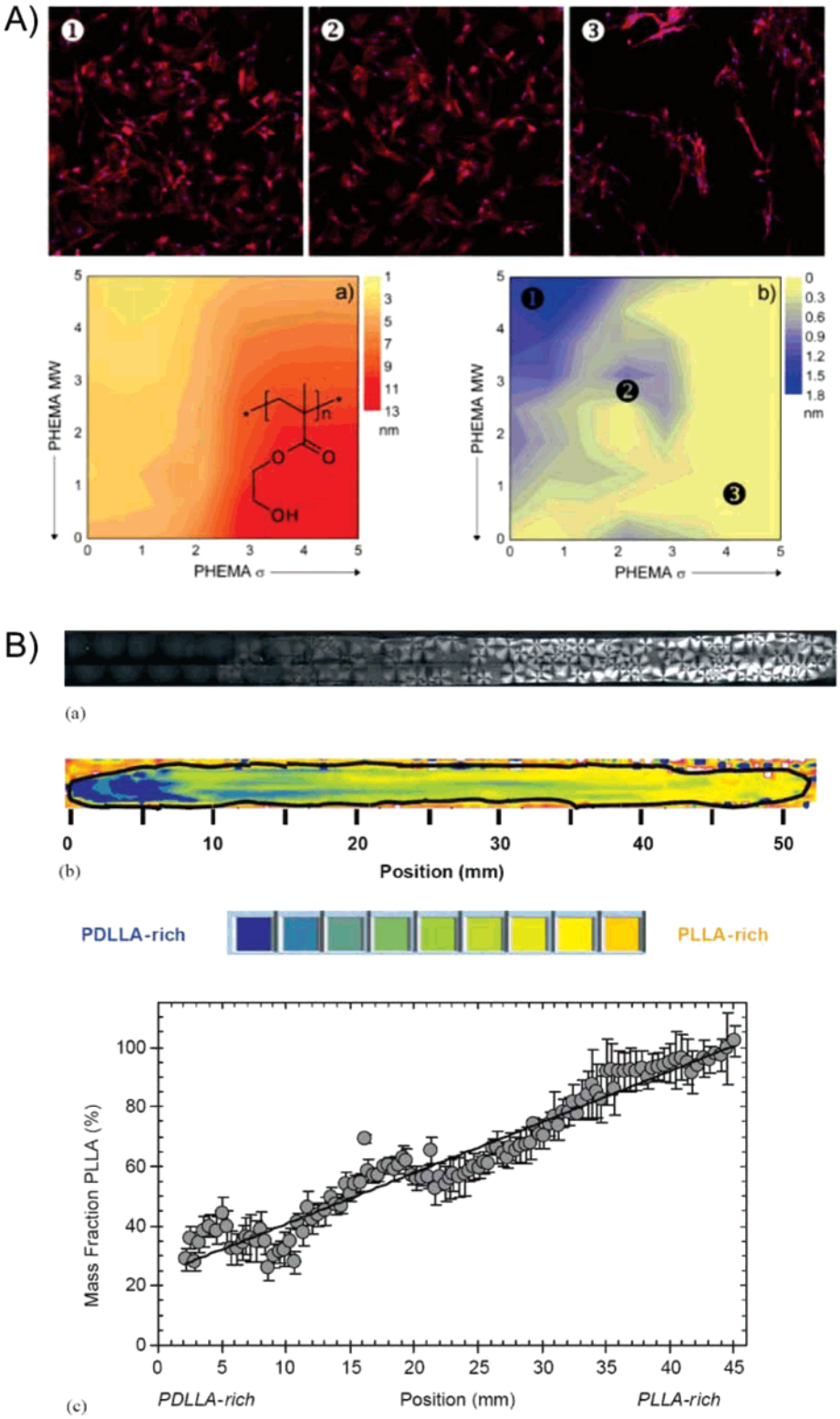

Figure 16. (A) Contour plots of (a) the dry thickness of poly(2-hydroxyethyl methacrylate) (PHEMA) in an MW/σ orthogonal PHEMA gradient (scale in nanometers) and (b) dry fibronectin (FN) thickness in an MW/σ orthogonal PHEMA/FN gradient (scale in nanometers). The scales depicting the position on the substrate in parts a and b are in centimeters. (Top) Images of MC3T3-E1 cells (nucleus, blue; cytoskeleton/actin, red) cultured on the PHEMA/FN gradient substrates. Images are recorded at positions on the sample marked with the numbers in the bottom panel[17] (reproduced with permission from Wiley). (B) Image of the birefringence from a poly(L-lactic acid) (PLLA)-poly(D-lactic acid) (PDLLA) gradient is shown. Forty-six overlapping images taken through crossed polarizers using transmitted light microscopy were assembled into the final image shown. The higher crystallinity of the PLLA-rich end of the gradient causes it to be more birefringent than the PDLLA-rich end. The gradient shown is 52 mm long. (b) FTIR-RTM (reflection−transmission) map of a PLLA-PDLLA composition gradient. The strip film has been outlined in black. A qualitative gradient in color is visible in the film, with blue corresponding to PDLLA-rich regions and orange corresponding to PLLA-rich regions. (See the color bar below the map.) Pixels located outside the black borders represent artifacts from bare regions on the slides and were not included in the composition calculations. (c) The compositions of six PLLA-PDLLA gradients determined with FTIR-RTM were averaged and plotted versus position[255] (reproduced with permission from Elsevier).

traversing gradient pathways over the past few years. We apologize to those whose research accomplishments we have failed to mention; it surely was not our intention. Please contact us and let us know about your exciting work so that we can properly update our existing database of gradient research projects. We express our sincere thanks to Sara Arvidson for carefully reading the manuscript and providing fruitful comments and suggestions. Finally, we gratefully acknowledge the financial support from several funding agencies, including the National Science Foundation, Henry & Camille Dreyfus Foundation, Office of Naval Research, Army Research Office, and Petroleum Research Fund, who have generously funded our research efforts in this field.

Note Added in Proof. During the typesetting of the article another review of gradient substrates appeared that described developments and application of such structures for biomadial applications (Kim, M. S.; Khang, G.; Lee, H. B. *Prog. Polym. Sci.* **2008**, *33*, 138−164).

LA7033164